

1 **This manuscript is contextually identical with the following published paper:**

2 Botta-Dukát Z; Czúcz B (2016) **Testing the ability of functional diversity indices to detect trait**
3 **convergence and divergence using individual-based simulation.** - METHODS IN ECOLOGY AND
4 EVOLUTION 7: (1) pp. 114-126. DOI: 10.1111/2041-210X.12450

5 **The original published PDF available in this website:**

6 <http://onlinelibrary.wiley.com/doi/10.1111/2041-210X.12450/abstract>
7

8

9 **Testing the ability of functional diversity indices to detect trait convergence and**
10 **divergence using individual-based simulation**

11

12 **Running title:** Detecting trait convergence and divergence

13

14 **Author:** Zoltán Botta-Dukát, Bálint Czúcz

15

16 **Manuscript length:** 8798 words

17

18 **Address:** MTA Centre for Ecological Research, Institute of Ecology and Botany, Alkotmány 2-4,

19 Vácrátót, H-2163, Hungary.

20 **E-mail:** botta-dukat.zoltan@okologia.mta.hu

21

22

23

24 **Summary**

- 25 1. The quest for ‘assembly rules’, i.e. the processes shaping the species composition of
26 communities, is a central issue in community ecology. Nevertheless, so far there is no general
27 agreement on a framework to detect assembly rules in real life data: several key elements
28 are still missing or heavily disputed, including the choice of the appropriate test statistic (e.g.
29 functional diversity index) and randomization strategy for each major assembly process.
- 30 2. Simulation studies based on artificial communities can help to explore the usefulness of
31 different approaches in detecting assembly rules. Nevertheless, the currently dominant
32 approach to simulate artificial communities (i.e. selecting species from a pool based solely on
33 trait values) oversimplifies the complex processes involved in community assembly and thus
34 fails to produce realistic patterns. Consequently, its value for testing methodologies is
35 seriously limited.
- 36 3. In this study we implemented a flexible, individual-based algorithm simulating real-life
37 community processes (individuals are born, survive, compete for resources, reproduce and
38 die), to generate artificial species composition data. With the help of this algorithm, we
39 estimated the type I error rates and the statistical power of five different diversity indices
40 (FRic, Rao’s quadratic entropy, FEve, the variance of functional distances, and the variance of
41 nearest neighbor distances) in combination with three randomization strategies
42 (randomization of trait values in the whole dataset, within plots and within the range of trait
43 values occurring in each plot) for detecting two underlying assembly processes (habitat
44 filtering and limiting similarity). We also tested the influence of all adjustable simulation
45 parameters on the simulation results in a sensitivity analysis framework.
- 46 4. The results of the sensitivity analysis show that the individual-based simulation framework
47 proposed here can be used for creating artificial community data with realistic pattern of

48 trait values. Based on the results, Rao's quadratic entropy performed best for detecting both
49 habitat filtering (trait convergence) and limiting similarity (trait divergence). Functional
50 richness may also be suitable for detect traiting convergence. Functional evenness and
51 variance of nearest neighbor distances, however, should not be used for finding assembly
52 rules.

53 **Keywords:** assembly rules, Type I error rate, statistical power, functional richness, functional
54 evenness, Rao's quadratic entropy

55

56 **Introduction**

57 Understanding the rules of community assembly from a regional species pool is a central issue in
58 community ecology (Keddy 1992). Assembly rules are constraints on species coexistence (Weiher *et al.*
59 *al.* 2011; Götzenberger *et al.* 2012) that predict species presence and abundance in the local
60 community (Keddy 1992). These constraints can be organized into a hierarchy of filters (Belyea &
61 Lancaster 1999; Götzenberger *et al.* 2012). In community assembly studies focusing at a small area
62 with negligible dispersal limitation, two such constraints are frequently considered. On one hand,
63 individuals have to survive and reproduce under the given environmental conditions; this filter is
64 often referred to as environmental (or habitat) filtering. On the other hand, species may be absent
65 from suitable habitats due to interspecific competition, which forms the second filter. Limiting
66 similarity theory (MacArthur & Levins 1967; Meszéna *et al.* 2006) predicts that species can only
67 coexist if they are regulated differently (e.g. use different resources). The theory was originally
68 developed in the context of resource competition, but there are several other potential stabilizing
69 mechanisms (Chesson 2000; Wilson 2011) that can be based on differences in species attributes.
70 Different approaches proposed to detect these two filters (i.e. habitat filtering and limiting similarity)
71 have been reviewed by Götzenberg *et al.* (2012). In the last few years, the trait-based approach

72 became dominant in this field. Habitat filtering and limiting similarity influence the distribution of
73 trait values in opposite ways (Mouillot *et al.* 2007; Cornwell & Ackerly 2009; Götzenberger *et al.*
74 2012). Habitat filtering leads to lower variation in trait values than random selection from the species
75 pool (i.e. trait convergence) by excluding trait values not adapted to the local conditions (Figure 1).
76 On the other hand, if coexisting species use different resources, they should differ markedly in the
77 related traits, thus exhibiting more variance in trait values than would be expected for a random
78 assembly (trait divergence).

79 Although trait convergence and divergence are two opposite patterns, habitat filtering and limiting
80 similarity may act simultaneously (Weiher *et al.* 2011). When using a single test statistic with just one
81 null-model, trait convergence and divergence are mutually exclusive outcomes (de Bello *et al.* 2012),
82 and the lack of significant departure from the null-model may even indicate a balance between these
83 two processes (Mason *et al.* 2008). Simultaneous effects of habitat filtering and limiting similarity can
84 be detected only using more than one null model (e.g. Bernard-Verdier *et al.* 2012) or test statistic
85 (Joner *et al.* 2012).

86 Although there is considerable evidence both for trait convergence and divergence, most of the tests
87 (72% in the meta-analysis by Götzenberg *et al.* 2012) report no significant departure from the null-
88 model. Possible reasons are that (i) the tested traits are neutral, (ii) the studied dataset is too small
89 to detect departures from randomness or (iii) the applied test statistics and/or null-models were
90 inappropriate. Indeed, there is no consensus on which test statistic and null-model should be used,
91 and the methods applied show large variation (see Appendix S1 for illustration).

92 Previous attempts to check the ability of functional diversity indices to distinguish between trait
93 convergence and trait divergence were based on algorithms that select species from the species pool
94 following trait-based rules (Mouchet *et al.* 2010; de Bello *et al.* 2012; Aiba *et al.* 2013; Mason *et al.*
95 2013). The disadvantage of this approach is that it does not try to simulate the real processes, but
96 only aims at reproducing the expected pattern (trait convergence or divergence). There is only one

97 study so far (Münkemüller et al. (2012) which applied a spatially explicit, individual-based modeling
98 strategy to simulate the real underlying community processes: i.e. individuals are born, survive,
99 compete for resources, reproduce and die. However, even this study applied a cellular-automaton
100 simulation model with only one individual in each cell, which means that one of the key processes
101 (limiting similarity) could not be tested.

102

103 The aim of this study is two-fold. We developed an individual-based simulation framework capable of
104 testing methods and hypotheses regarding assembly rules and tested the general applicability of this
105 framework. Secondly we evaluated the ability of functional diversity indices to detect habitat filtering
106 and limiting similarity, using artificial data from the simulations.

107

108 **Methods**

109 *Individual based simulation*

110 We simulate the species composition of a set of locations along an environmental gradient using
111 individual-based simulation (Black & McKane 2012). The simulation operates on an ecological time-
112 scale; the regional species pool defined in the beginning does not change during the simulation. Each
113 species is characterized by the values of three numerical traits: trait A is related to habitat matching,
114 trait B regulates resource acquisition, while trait C is neutral. There is no within-species variation in
115 trait values. Individuals compete for space and resources. Competition for space is strict: for each
116 local community, the total number of individuals is limited, and a new individual can enter only after
117 another resident has died. Competition between individuals depends on their similarity in traits
118 related to resource acquisition; thus the competition is symmetric and it is strongest between
119 conspecifics,. The slope of the “difference in trait B” vs.” strength of competition” curve depends on
120 parameter σ_B (width of the competition kernel) with lower values resulting in a steeper slope, and if

121 $\sigma_B=0$, only individuals with the same trait values compete (in practice, this means that there is no
122 interspecific competition). In addition to competition, the vital rates of a species are also determined
123 by its how well it is adapted to the local conditions. The adaptedness is set to be different for
124 different environmental conditions, depending on the difference between the position of local
125 community along the environmental gradient and the value of trait A for the species. Thus each
126 location along the environmental gradient favors a different value in trait A, and the survival
127 probability of seedlings decreases with increasing difference between the actual and the locally
128 optimal trait value. The speed of this decrease depends on the parameter σ_A (the strength of
129 filtering) with lower values resulting in a steeper decrease. If $\sigma_A=\infty$, survival rates become constant.
130 Local communities are not isolated, thus there is a continuous propagule inflow from the other local
131 communities with a low rate. The model is not spatiality explicit, so the position of the individuals
132 within the community does not influence competition, and the position of the communities does not
133 influence propagule exchange. Nevertheless, as we consider each local community to be represented
134 by one “plot” (a sample from a specific location at a specific position of the gradient) that contains
135 only the entire local community, we use the terms “plot” and “local community” as synonyms in this
136 study.

137 The simulation consists of a community initialization followed by an iterative simulation of a
138 “disturbance-regeneration” cycle. The main steps of the simulation are illustrated in Figure 2, and
139 explained in detail in Appendix S2. The parameters regulating the simulation algorithm and their
140 values are shown in Table 1.

141

142 *Functional diversity indices*

143 Functional diversity is a complex concept, which is composed of three primary components:
144 functional richness, functional divergence and functional evenness (Mason *et al.* 2005; Villéger *et al.*
145 2008). It is expected that habitat filtering and limiting similarity influence different components of
146 functional diversity (Ravel *et al.* 2012): habitat filtering decreases the functional richness (by

147 excluding non-adapted species) and functional divergence (due to higher abundance of optimally
148 adapted species), while limiting similarity increases functional divergence and functional evenness by
149 increasing the difference between dominant species (Figure 1). These expectations fit well into the
150 theoretical framework developed by Boulangeat et al. (2012): species are first filtered by the abiotic
151 environment which may be followed by further exclusions due to competition, and the abundance of
152 occurring species are determined by competition and environmental filtering acting together.
153 We selected five indices for testing based on the comprehensive review of Pavoine and Bonsall
154 (2011) so as to represent all three components of functional diversity: richness, divergence and
155 evenness. We focused on indices calculated from distance matrices, as these are also applicable in
156 phylogenetic studies, and offer a relatively straightforward way for incorporating intraspecific trait
157 variation (de Bello *et al.* 2013a). Nevertheless, as there is no widely accepted distance-based
158 measure of functional richness, and because it is known to be a good indicator of habitat filtering
159 (e.g. Cornwell *et al.* 2006), we also examined the convex hull volume – which is thus the single metric
160 in this study that is calculated directly from trait values. Information on the selected indices is
161 summarized in Table 2.

162 Although distance-based indices can be used to quantify a multivariate functional diversity based on
163 several traits at the same time, we still tested each trait separately. There are several reasons for this
164 decision. Including all traits into a single analysis may hide existing patterns: opposite departures
165 from randomness (i.e. convergence and divergence) in different traits may cancel each other out
166 (Spasojevic & Suding 2012), while including neutral traits weakens the statistical tests (Butterfield &
167 Suding 2013).

168

169 *Null-models*

170 Many different randomization algorithms have been used in trait-based assembly rules studies. Since
171 the scope of the present study was testing functional diversity indices, not randomization algorithms,
172 only three such algorithms were applied (Table 3). The first one involves reshuffling trait values

173 among the species in the whole dataset containing all of the local communities (hereafter called
174 “between-plots” randomization strategy). Note that this reshuffling is essentially equivalent to
175 randomly drawing species from the pool of observed species (e.g. Cornwell *et al.* 2006; Montaña *et*
176 *al.* 2014). The between-plot randomization strategy assumes a null-model that any species can occur
177 in any local community with any abundance. This means that both habitat filtering and limiting
178 similarity can cause departures from the random pattern.

179 In the second algorithm species traits are shuffled among the species occurring at each plot
180 separately (hereafter called “within-plot” randomization strategy). This strategy relies on the
181 inherent assumption that the occurrence of species is already determined by environmental filtering,
182 but their abundance can still be shaped by interspecific competition. This strategy is furthermore
183 equivalent to randomizing abundances among the species present, a null-model applied for example
184 by Mason *et al.* (2008, 2013) and Pakeman *et al.* (2011). In the within plot randomization strategy the
185 null hypothesis is that any of the occurring species could be dominant; functional divergence (i.e.
186 larger than expected dissimilarities between the most abundant species) is a consequence of limiting
187 similarity.

188 The third randomization strategy is reshuffling abundances within the environmentally filtered pool
189 (hereafter called “restricted” randomization) that is, among species whose trait values fall within the
190 range of observed trait values in a community (Cornwell & Ackerly 2009). This null-model
191 hypothesizes that environmental filtering excludes species with trait values outside from this range,
192 but the occurrence and abundance of the non-excluded species are independent from their trait values.

193

194 The distribution of the functional diversity indices under the null models were characterized by their
195 values in 999 independent randomizations. One-sided tests were applied, which means that p-values
196 (probability of type I error) were calculated separately for trait convergence (in the between-plot
197 randomization strategy only) and divergence hypotheses (in all randomization strategies).

198

199 *Simulation experiments*

200 To test the effect of the different parameters on the simulated communities, we applied a sensitivity
201 analysis consisting of 243 simulation experiments. These experiments were following a 3^{11-6} fractional
202 factorial design constructed with the help of the R package *planor* (Kobilinsky *et al.* 2014). We used
203 the parameter values shown in Table 1, which generally involved taking a baseline value, reducing it
204 by 33% and increasing it by 50% thus forming a geometric series of three values for the sensitivity
205 analysis. In the case of σ_A and σ_B , we only used the first three values in Table 1. We quantified all of
206 the functional diversity indices for all of the null models, interpreting the type I error rates and the
207 power of the tests (see below) as goodness metrics revealing the appropriateness of the simulation
208 setup (parameter values) for use in evaluating functional diversity indices.

209 As an additional exercise to explore the consequences of no habitat filtering and/or competition in
210 the simulation, we performed a further 4x4x3x3 full factorial experiment using all values of σ_A , σ_B ,
211 the number of species in the regional species pool (S) and the number of individuals in a local
212 community (J), and the baseline values (i.e. first value in Table 1) of all other parameters from Table
213 1. The impact of the key parameters σ_A (the strength of environmental filtering) and σ_B (width of the
214 competition kernel) on the simulation is further explored in Appendix S2.

215

216 *Evaluation of the results of randomization tests*

217 The randomization tests resulted in one p-value for each local community. The proportion of p-
218 values lower than 5% was calculated for each meta-community. These proportions (interpreted as
219 type I error or power depending on the parameters) were used in the subsequent analysis. We first
220 checked whether the rate of type I errors (the proportion of significant results if there is no effect) is
221 equal to the predefined significance level in two different ways: (1) by switching off filtering and/or
222 competition by setting $\sigma_A = \infty$ or $\sigma_B = 0$ respectively, or (2) by testing the neutral trait the value of
223 which did not influence the community assembly. Then we estimated the power of the test, i.e. the
224 proportion of significant results, when there is a known direct effect. The effect of the simulation

225 parameters on the type I error rate and power were explored by fitting classification tree models to
226 the results from the fractional factorial experiment. We fitted conditional, inference-based
227 classification trees for this purpose using the ctree algorithm implemented in the “party” package in
228 R (Hothorn *et al.* 2006). The big advantage of ctree over most of the traditional classification and
229 regression tree (CART) algorithms (e.g. Breiman *et al.* 1984) is that ctree offers unbiased variable
230 selection and a statistically sound stopping rule (Hothorn *et al.* 2006), thus the fitted models offer an
231 easily interpretable yet statistically sound ‘decision key’ for selecting the optimal algorithm in
232 different study contexts. To offer insight into the selection of appropriate functional diversity indices,
233 we also included the type of the test statistic as an explanatory variable into the ctree models. As the
234 dependent variable, we used the proportion of power above 0.8, an arbitrary, but widely used
235 threshold for power (like 0.05 for significance levels). Separate analyses were done for the three
236 randomization methods. Similar ctree models were also fit to compare alternative methods for
237 detecting the same process in order to guide future field-based studies. We used the difference in
238 power as the dependent variable and parameters which can be determined from field data, including
239 alpha- and beta-diversity, as predictors in these ctree models.
240

241 **Results**

242 *General overview and Type I error rates*

243 The communities constructed with the simulation algorithm exhibited general community structures
244 very similar to real life plant communities: the mean species richness of local communities (alpha
245 diversity) ranged from 4.7 to 57.7 (mean: 21.2), and the total number of species in the final
246 simulation results (gamma diversity) was between 7 and 300 (mean: 89.6), which lead to beta-
247 diversity values (i.e. the ratio of gamma- and alpha-diversity) ranging from 1.1 to 20.3 (mean: 4.635).
248 The distributions of the traits in the simulation results differed from their distribution in the initial
249 regional species pool in the expected way (Appendix S3).

250 For the in between- and within-plot randomizations, the type I error rates did not differ significantly
251 from the predefined 5% threshold the vast majority of the test cases (Figure 3), while they often
252 greatly exceeded the predefined threshold in restricted randomization. The cumulative distributions
253 of type I error rates estimated in the two ways (i.e. by switching off both effects or by using neutral
254 traits) did not differ considerably (Figure S4.1).

255

256 *Power for detecting trait convergence due to habitat filtering*

257 Only FRic and RaoQ had acceptable power in some (but not all) parameter combinations (Figure 4).
258 The power of the other indices was generally low (i.e. below 0.8) for all combinations of the
259 simulation parameters. Not surprisingly, the strength of habitat filtering in the simulated
260 communities strongly influenced the power of the tests (Figure S4.2). Setting up the ctree model for
261 *FRic* and *RaoQm* we found that the only simulation parameters which significantly influenced the
262 detectability of trait convergence in the parameter space explored were the strength of filtering (σ_A),
263 the width of the competition kernel (σ_B), and the correlation between traits A and B (c) (Figure 5).
264 RaoQ performed much better than FRic, if habitat filtering is weak, while FRic has slightly higher
265 power if the habitat filtering is strong. Using diversity values to predict differences between the
266 power of the two functions, we found that RaoQ is preferable if local richness is high, while beta

267 diversity is relatively low. Any correlation between the traits related to habitat filtering and
268 competition decreases the detectability of habitat filtering, irrespective of its sign.

269

270 *Power for detecting trait divergence due to competition*

271 For trait divergence, we observed a generally low power of detection for all indices and
272 randomization strategies. There was a low power of detection using the between-plot randomization
273 strategy for trait divergence, and only *RaoQ* and the variance of differences (*Vd*) exceeded the
274 threshold value in some cases (Figure 4.b). Not surprisingly, the parameters fine-tuning the
275 competition process (i.e. σ_B and K) significantly influenced the detection rate, but the probability of
276 reaching a high level of power remained low, even when competition was strong (Figure 5.b). *RaoQ*
277 performed better than *Vd* if beta diversity was low (i.e. in a less heterogeneous environment where
278 habitat filtering plays a minor role, Figure S4.4). Furthermore, the lack of habitat filtering significantly
279 improved the power of *RaoQ* but not the other indices (Figure S4.5).

280 We also experienced low power levels for the within-plot randomization strategy with *RaoQ* being
281 the only index which gave some above threshold cases (Figure 4.c). *RaoQ* was better at detecting
282 intraspecific competition when the local communities were larger (high J , Figure 5.c).

283 In restricted randomization, *FRic* and *RaoQ* gave a relatively high power (Figure 4.d), but this came at
284 the price of a high type I error rate, compromising the practical applicability of this randomization
285 strategy.

286 Within plot randomization performed the best of the two randomization strategies, with acceptable
287 type I error rates for *RaoQ*. It exhibited significantly higher overall power than the between-plot
288 strategy (median difference is 0.06; $p < 0.001\%$, with a Wilcoxon paired rank sum test). Nevertheless,
289 there were also several cases when between-plot randomization performed better (Figure S4.6), and
290 the difference between the two methods could not be predicted by the diversity values.

291

292 **Discussion**

293 *Functional richness and quadratic entropy indicate habitat filtering*

294 Habitat filtering is expected to restrict the range of trait values and thus decrease the functional
295 richness (Weiher *et al.* 1998; Cornwell *et al.* 2006). For this reason, habitat filtering is often
296 considered to be indicated by lower than expected *FRic* values (e.g. Cornwell *et al.* 2006; Bernard-
297 Verdier *et al.* 2012; Raavel *et al.* 2012). Our results pointed out that this relationship strongly
298 depends on the environmental heterogeneity of the datasets studied (Willis *et al.* 2010; de Bello
299 2012): the power of the tests becomes low if the gradient sampled is short relative to the tolerance
300 width of the species (Figure 5). With low environmental heterogeneity, trait values get filtered
301 almost the same way in all plots. Thus there is no considerable difference to be expected in their
302 plot level minimum and maximum values, and consequently in the actual and expected values of
303 *FRic*.

304 As Rao's quadratic entropy is expected to combine functional richness and functional divergence
305 (Mouchet *et al.* 2010), its use for detecting a decrease in functional richness due to habitat filtering is
306 justified. According to Raavel *et al.* (2012), environmental filtering may influence not only the range
307 of trait values, but also the position of dominant species in the trait space (functional divergence
308 sensu Villéger *et al.* 2008). Rao's quadratic entropy is influenced by both effects, which may be
309 advantageous when the aim is the detection of environmental filtering. And yet, even though *RaoQ*
310 may also be influenced by limiting similarity, we found it highly appropriate for detecting habitat
311 filtering, too. One possible explanation for the superior performance of *RaoQ* is that it is less
312 sensitive to extreme trait values than *FRic* (Cornwell & Ackerly 2009). In a multi-trait analysis, the
313 usage of *RaoQ* can also help to avoid the problems associated with convex hull volume discussed by
314 Podani (2009).

315

316 *Detecting limiting similarity remained an unresolved problem*

317 None of the indices that we tested proved unequivocally appropriate for detecting limiting similarity.
318 Even the best performing, Rao's quadratic entropy (*RaoQ*) and variance of distances (*Vd*) indices, had

319 relatively low statistical power using any randomizations with reasonable type I error rates. The
320 theoretical minimum value of Vd is attained if the species are placed equidistantly in the trait space,
321 thus relatively low values can emerge due to interspecific competition which is supposed to
322 homogenize the size of gaps among species in the trait space. The low power of this test statistic may
323 accordingly be explained by the fact that Vd does not use the abundances, and even a small number
324 of non-complying rare species may break the even spacing of trait values. Another possible
325 explanation could be that the range of Vd is highly sensitive to the range of trait values (that is $FRic$),
326 which is, on the other hand, highly influenced by habitat filtering (Appendix S5). Nevertheless, the
327 fact that the power of Vd is not sensitive to the strength of habitat filtering, and RaoQ outperforms
328 Vd at low beta diversity (i.e. in homogeneous environments where habitat filtering plays a minor
329 role) contradicts the latter explanation.

330 As we have already discussed, $RaoQ$ combines aspects of functional richness (i.e. the range of trait
331 values) and functional divergence (i.e. the position of dominant species relative to the center of trait
332 range). It seems highly improbable that limiting similarity would influence $RaoQ$ values through
333 altering functional richness (Cornwell & Ackerly 2009; Bernard-Verdier *et al.* 2012). Under what
334 conditions can limiting similarity lead to high functional divergence? Functional divergence is high if
335 abundant species are situated near the border of the occupied trait space. Limiting similarity predicts
336 that dominant species are situated as far as possible from one another in the trait space. When
337 considering only one trait, functional divergence is maximal if dominant species are situated at the
338 two opposite ends of the trait gradient. This is in agreement with the pattern expected due to
339 limiting similarity for two dominant species but contradicts the expected equidistant spacing of
340 dominants if there are more than two dominant species. Note that increasing the dimensionality of
341 the trait space can increase the number of dominant species that can be placed near the border and
342 far from each other at the same time. Thus functional divergence measures (including $RaoQ$)
343 probably perform better in multi-trait studies. The dimensionality of the trait space can be higher

344 than the number of traits for nominal (multistate) traits or when the overlap of trait distribution is
345 used as distance measure (de Bello *et al.* 2013a).

346 Contrary to what its name suggests, *FEve* (“functional evenness index”) was unsuitable for detecting
347 limiting similarity. One possible explanation is that *FEve* considers only neighbors in trait space (true
348 neighbors in the unidimensional space of our tests, which is generalized as a minimum spanning tree
349 in the multidimensional case), while limiting similarity predicts that dominant species highly differ in
350 traits (**Hiba! A hivatkozási forrás nem található.**Figure 6).

351 The variance (or standard deviation) of nearest neighbor distances (*Vnnd*) is another metric
352 frequently used to detect limiting similarity in studies with real data, but which did not work well for
353 this purpose in our simulations. This index is often successfully used to detect even spacing of species
354 along a trait axis, which is interpreted as a result of limiting similarity (e.g. Cornwell & Ackerly 2009;
355 Katabuchi *et al.* 2012). Nevertheless, *Vnnd* is similar to *FEve* in that only neighboring trait values are
356 considered. Accordingly, many fundamentally different patterns may result in the same *Vnnd* value
357 (Figure 6), which might explain the poor performance of this popular and seemingly well-suited
358 metric. Based on our negative test results, we suggest that neither *Vnnd* nor *FEve* should be used to
359 detect limiting similarity or trait divergence.

360

361 *A quest for appropriate randomization strategies*

362 All of the available randomization strategies test null hypotheses that slightly differ from the
363 theoretical hypotheses that can be deduced from the processes (Figure 1). When testing for the
364 effects of environmental filtering, the trait distribution in the local community should be compared
365 with that of a community assembled randomly from the regional species pool. The between-plot
366 strategy comes close to this, but it uses the pool of the species “observed” (i.e. set of species
367 occurring in at least one plot) instead of the entire regional pool. If all local communities sampled are
368 assembled from the same regional pool (i.e. the dispersal limitation is negligible), the pool of
369 observed species is a subset of the regional pool. If a lot of local communities are sampled, and they

370 cover the whole range of environmental variability within the region, the difference between the two
371 sets is small. This small difference explains the high power of between-plot randomization to detect
372 environmental filtering, when a wide range is sampled along the environmental gradient.

373 For testing limiting similarity, the actual trait distribution in the local community should be compared
374 to that of a community randomly assembled from the “environmental” species pool, i.e. the species
375 that can theoretically occur under the given environmental conditions. Between-plot randomization
376 uses the set of species occurring in the whole dataset instead of the environmental species pool. If
377 the dataset consists of local communities from different environments, it can contain a lot of species
378 that do not belong to the environmental species pool. The more environmentally homogeneous the
379 dataset is, the less difference there is between the two sets of species. Within-plot randomization, on
380 the other hand, uses the list of species that actually occur in the tested community instead of
381 environmental species pool. In contrary to between-plot randomization, this set is narrower than it
382 should be (i.e. all species occurring in the local community belong to the environmental pool, but
383 many of species from the environmental pool may be absent, including the species actually filtered
384 out by competition). This is a significant shortcoming when using plot simulations to test for limiting
385 similarity, which can explain why we saw low power with within-plot randomization. The
386 detectability of limiting similarity could be improved by using a randomization strategy with a
387 reference set closer to the environmental pool (Cornwell & Ackerly 2009; de Bello *et al.* 2012).

388 Restricted randomization aims at defining a more plausible environmental pool using the range of
389 observed trait values as the reference set. However, this definition resulted in high type I error rate
390 for indices influenced by range of traits, i.e. FRic and RaoQ. To understand this shortcoming, one
391 should consider that the range of trait values can never be higher in the random communities
392 created by restricted randomization than in the observed one. If the value of a functional diversity
393 index depends on the trait range, this restriction obviously leads to an artificial “trait divergence” (i.e.
394 higher observed value than mean of random values) even in neutral communities. Therefore we
395 suggest that this way of creating an environmentally filtered pool for randomization should be

396 avoided if possible. Nevertheless, this limitation is not important when the filtered pool is
397 constructed through spatial scaling (Swenson *et al.* 2006) or based on species habitat preference (de
398 Bello *et al.* 2012), or if species are selected with probabilities depending on the suitability of local
399 habitat (Chalmandrier *et al.* 2013). Since the novel concept of dark diversity (Pärtel *et al.* 2011) is
400 defined as the species absent from the local community but belong to the environmentally filtered
401 pool, methods for estimating dark diversity, e.g. Beals smoothing (Ewald 2002; Botta-Dukát 2012),
402 may also be useful for testing limiting similarity.

403

404 *Detectability of assembly rules*

405 In the meta-analysis of Götzenberg *et al.* (2012) only 358 of the 1966 tests reviewed (18%) showed
406 significant departures from randomness. One possible reason for this low proportion is that the
407 applied statistical tests have low power. Our simulations confirmed that some of the widely used test
408 statistics have low power. Therefore we suggest that non-significant results found in such studies
409 should be, if possible, re-analyzed using more powerful statistical tests.

410 64% of the significant tests examined by Götzenberg *et al.* (2012) had divergence of trait values that
411 seems to contradict our results on the low power of tests dedicated to detecting trait divergence.

412 However, a test level meta-analysis may be biased by case studies from homogeneous environments
413 with a high number of tests, where the effect of environmental filtering is hardly detectable

414 (examples of such studies are Stubbs & Wilson 2004; Mason & Wilson 2006). Aggregating results at

415 the level of studies could show the opposite pattern. Merging the data collected by Emerson &

416 Gillespie (2008: Table 1), Vamosi *et al.* (2009: Table 1) and HilleRisLambers *et al.* (2012: Table 1), 33

417 studies find trait or phylogenetic convergence, 11 studies find divergence, and 22 studies find both.

418 We think these numbers mirror the higher detectability of environmental filtering, which is in line

419 with our results.

420

421 *A niche for individual-based simulations*

422 There is a broad variety of methods developed for detecting assembly rules. As this study
423 exemplifies, checking the statistical power of the methods is necessary even if they seem to be well-
424 established theoretically. The individual-based simulation framework introduced in this paper can be
425 a useful tool for such studies. The simulation presented in this paper was developed in R, a widely
426 used high-level statistical scripting language, and the source code is available in Appendix S6.

427 This study focused on a very limited set of popular distance-based functional diversity indices. The
428 broad spectrum of available test statistics is worth a deeper investigation with individual-based
429 simulation models. Other functional or phylogenetic diversity indices (Pavoine & Bonsall 2011) or test
430 statistics unrelated to the concept of functional diversity (e.g. Pillar *et al.* 2009; Shipley *et al.* 2012; de
431 Bello *et al.* 2013b; Shipley 2014) are less widely used, but they could potentially highly outperform
432 the ones studied in this paper. A systematic analysis of all available choices within a well-designed
433 IBM environment would undoubtedly offer major methodological guidance for field studies.

434 We focusing primarily on the performance of the test statistics, so we applied only three widely used
435 randomization strategies. There are several more possible randomization approaches, an exhaustive
436 testing of which would also be necessary, with special regard for methods appropriate for detecting
437 limiting similarity.

438 The individual-based simulation model presented in this paper is an attempt at constructing a
439 minimal in silico representation of two major processes shaping the composition of ecological
440 communities: habitat filtering and limiting similarity. Nevertheless, such a model is necessarily
441 incomplete, and the model can be refined for producing a more realistic representation at the price
442 of adding more complexity to the simulation. In the present version, there is no within-species
443 variation in trait values, but this property can be implemented in a relatively simple and
444 straightforward way within this framework. If individuals differ not only in their traits within the
445 species, but this difference is also heritable, the simulation framework can potentially be made
446 suitable for studying evolutionary processes.

447 Beyond environmental filtering, there may be alternative processes that lead to trait convergence.
448 The most important such processes are asymmetric competition (Mayfield & Levine 2010) and
449 dispersal limitation (Münkemüller *et al.* 2012). Both of these complexities can potentially be
450 incorporated into this simulation framework. Competition can be made asymmetric by replacing
451 Equation 3 in Appendix S2 with the formula of Kisdi (Kisdi 1999), whereas spatially limited dispersal
452 can be generated relatively easily after setting up a spatial neighborhood or distance matrix for the
453 local communities in step 4 (Appendix S2). Nevertheless, the power of methods for detecting the
454 effect of spatial pattern of environment and limited dispersal were exhaustively studied by
455 Münkemüller *et al.* (2012) using cellular automaton simulation, an approach which might be better
456 suited to studying spatial processes, but which cannot easily handle limiting similarity with only one
457 individual living in each cell.

458 In addition to checking the applicability of methods for detecting assembly rules, a similar simulation
459 framework could also be useful for exploring the factors influencing the alpha-, beta- and gamma-
460 diversity of artificial communities. Such exploration would give new insight into the relative
461 importance of stochastic and deterministic processes in community organization, which has been a
462 highly debated subject in the last few years (Chase & Myers 2011; Gravel *et al.* 2011; Rosindell *et al.*
463 2012; Vellend *et al.* 2014).

464

465 **Conclusions**

466 Of the functional diversity indices studied, Rao's quadratic entropy seems to be most suitable for
467 testing for both trait convergence (due to environmental filtering) and trait divergence (due to
468 limiting similarity). Environmental filtering can be detected relatively reliably using the between-plot
469 randomization strategy, if the data set covers a wide range of environmental conditions. If an
470 environmentally homogeneous area was sampled, however, trait convergence can become
471 impossible to detect without using external information on the regional species pool, because the
472 species "filtered out" by the unsuitable environment are absent from the entire dataset.

473 None of the combinations of diversity indices and randomization strategies tested can reliably detect
474 trait divergence due to limiting similarity under all conditions. . However, if there is a lack of habitat
475 filtering (i.e. if the dataset is environmentally homogeneous), Rao's quadratic entropy combined with
476 a between-plot randomization strategy can detect this process.

477 For existing datasets, the ability to detect habitat filtering may be improved by increasing the
478 environmental heterogeneity of the dataset. On the other hand, analyzing data from a narrow range
479 of environmental variables increases the detection probability of limiting similarity.

480 In the light of the outcomes of our simulations, non-significant results in studies with real-data
481 should be interpreted very carefully. In addition to the lack of the effect tested, negative results can
482 occur in several ways ranging from the masking of limiting similarity by environmental filtering to the
483 inability of the chosen index/test to detect an existing effect. As we have shown, several seemingly
484 very well-suited and commonly used indices might be useless under experimental circumstances
485 with artificial data.

486

487 **Acknowledgement**

488 This research was supported by OTKA K83595 and K91180 research grants. Bálint Czúcz was
489 supported by the János Bolyai research fellowship of the Hungarian Academy of Sciences. We thank
490 Francesco de Bello, Lars Götzenberg, Imelda Somodi, and three anonymous reviewers for their
491 valuable comments, and Emily Rauschert for improving English language of the article.

492

493 **Data accessibility**

494 No real data were used in this paper. Simulation algorithm is available in form of R script in the
495 Supporting Information.

496

497 **Literature**

- 498 Aiba, M., Katabuchi, M., Takafumi, H., Matsuzaki, S.S., Sasaki, T. & Hiura, T. (2013). Robustness of
499 trait distribution metrics for community assembly studies under the uncertainties of
500 assembly processes. *Ecology*, **94**, 2873–2885.
- 501 de Bello, F. (2012). The quest for trait convergence and divergence in community assembly: are null-
502 models the magic wand? *Global Ecology and Biogeography*, **21**, 312–317.
- 503 de Bello, F., Carmona, C.P., Mason, N.W.H., Sebastia, M.-T. & Leps, J. (2013a). Which trait
504 dissimilarity for functional diversity: trait means or trait overlap? *Journal of Vegetation
505 Science*, **24**, 807–819.
- 506 de Bello, F., Price, J.N., Münkemüller, T., Liira, J., Zobel, M., Thuiller, W., Gerhold, P., Götzenberger,
507 L., Lavergne, S., Lepš, J., Zobel, K. & Pärtel, M. (2012). Functional species pool framework to
508 test for biotic effects on community assembly. *Ecology*, **93**, 2263–2273.
- 509 de Bello, F., Vandewalle, M., Reitalu, T., Lepš, J., Prentice, H.C., Lavorel, S. & Sykes, M.T. (2013b).
510 Evidence for scale- and disturbance-dependent trait assembly patterns in dry semi-natural
511 grasslands. *Journal of Ecology*, **101**, 1237–1244.
- 512 Belyea, L.R. & Lancaster, J. (1999). Assembly rules within a contingent ecology. *Oikos*, **86**, 402–416.
- 513 Bernard-Verdier, M., Navas, M.-L., Vellend, M., Violle, C., Fayolle, A. & Garnier, E. (2012). Community
514 assembly along a soil depth gradient: contrasting patterns of plant trait convergence and
515 divergence in a Mediterranean rangeland. *Journal of Ecology*, **100**, 1422–1433.
- 516 Black, A.J. & McKane, A.J. (2012). Stochastic formulation of ecological models and their applications.
517 *Trends in Ecology & Evolution*, **27**, 337–345.
- 518 Botta-Dukát, Z. (2012). Co-occurrence-based measure of species' habitat specialization: robust,
519 unbiased estimation in saturated communities. *Journal of Vegetation Science*, **23**, 201–207.
- 520 Botta-Dukát, Z. (2005). Rao's quadratic entropy as a measure of functional diversity based on
521 multiple traits. *Journal of Vegetation Science*, **16**, 533–540.
- 522 Boulangeat, I., Gravel, D. & Thuiller, W. (2012). Accounting for dispersal and biotic interactions to
523 disentangle the drivers of species distributions and their abundances. *Ecology Letters*, **15**,
524 584–593.
- 525 Breiman, L., Friedman, J., Ohlsen, R. & Stone, C. (1984). *Classification and regression trees*. Chapman
526 Hall/CRC Press, New York.
- 527 Butterfield, B.J. & Suding, K.N. (2013). Single-trait functional indices outperform multi-trait indices in
528 linking environmental gradients and ecosystem services in a complex landscape. *Journal of
529 Ecology*, **101**, 9–17.
- 530 Chalmandrier, L., Münkemüller, T., Gallien, L., de Bello, F., Mazel, F., Lavergne, S. & Thuiller, W.
531 (2013). A family of null models to distinguish between environmental filtering and biotic
532 interactions in functional diversity patterns. *Journal of Vegetation Science*, **24**, 853–864.
- 533 Chase, J.M. & Myers, J.A. (2011). Disentangling the importance of ecological niches from stochastic
534 processes across scales. *Philosophical Transactions of the Royal Society B: Biological Sciences*,
535 **366**, 2351–2363.

- 536 Chesson, P. (2000). Mechanisms of maintenance of species diversity. *Annual Review of Ecology and*
537 *Systematics*, **31**, 343–366.
- 538 Clarke, K. & Warwick, R. (2001). A further biodiversity index applicable to species lists: variation in
539 taxonomic distinctness. *Marine Ecology-Progress Series*, **216**, 265–278.
- 540 Cornwell, W.K. & Ackerly, D.D. (2009). Community assembly and shifts in plant trait distributions
541 across an environmental gradient in coastal California. *Ecological Monographs*, **79**, 109–126.
- 542 Cornwell, W.K., Schwilk, D.W. & Ackerly, D.D. (2006). A trait-based test for habitat filtering: convex
543 hull volume. *Ecology*, **87**, 1465–1471.
- 544 Emerson, B.C. & Gillespie, R.G. (2008). Phylogenetic analysis of community assembly and structure
545 over space and time. *Trends in Ecology & Evolution*, **23**, 619–630.
- 546 Ewald, J. (2002). A probabilistic approach to estimating species pools from large compositional
547 matrices. *Journal of Vegetation Science*, **13**, 191–198.
- 548 Götzenberger, L., de Bello, F., Bråthen, K.A., Davison, J., Dubuis, A., Guisan, A., Lepš, J., Lindborg, R.,
549 Moora, M., Pärtel, M., Pellissier, L., Pottier, J., Vittoz, P., Zobel, K. & Zobel, M. (2012).
550 Ecological assembly rules in plant communities—approaches, patterns and prospects.
551 *Biological Reviews*, **87**, 111–127.
- 552 Gravel, D., Guichard, F. & Hochberg, M.E. (2011). Species coexistence in a variable world. *Ecology*
553 *Letters*, **14**, 828–839.
- 554 HilleRisLambers, J., Adler, P.B., Harpole, W.S., Levine, J.M. & Mayfield, M.M. (2012). Rethinking
555 Community Assembly through the Lens of Coexistence Theory. *Annual Review of Ecology,*
556 *Evolution, and Systematics*, **43**, 227–248.
- 557 Hothorn, T., Hornik, K. & Zeileis, A. (2006). Unbiased Recursive Partitioning: A Conditional Inference
558 Framework. *Journal of Computational and Graphical Statistics*, **15**, 651–674.
- 559 Joner, F., Anand, M. & Pillar, V. (2012). Trait-convergence and divergence assembly patterns in a
560 temperate forest herbaceous layer along the gradient of canopy closure. *Community Ecology,*
561 **13**, 178–184.
- 562 Katabuchi, M., Kurokawa, H., Davies, S.J., Tan, S. & Nakashizuka, T. (2012). Soil resource availability
563 shapes community trait structure in a species-rich dipterocarp forest. *Journal of Ecology*, **100**,
564 643–651.
- 565 Keddy, P.A. (1992). Assembly and response rules: two goals for predictive community ecology.
566 *Journal of Vegetation Science*, **3**, 157–164.
- 567 Kisdi, É. (1999). Evolutionary Branching under Asymmetric Competition. *Journal of Theoretical*
568 *Biology*, **197**, 149–162.
- 569 Kobilinsky, A., Bouvier, A. & Monod, H. (2014). *PLANOR: an R package for the automatic generation*
570 *of regular fractional factorial designs. R package.*
- 571 Laliberté, E. & Legendre, P. (2010). A distance-based framework for measuring functional diversity
572 from multiple traits. *Ecology*, **91**, 299–305.

- 573 MacArthur, R. & Levins, R. (1967). The Limiting Similarity, Convergence, and Divergence of Coexisting
574 Species. *The American Naturalist*, **101**, 377–385.
- 575 Mason, N.W.H., de Bello, F., Mouillot, D., Pavoine, S. & Dray, S. (2013). A guide for using functional
576 diversity indices to reveal changes in assembly processes along ecological gradients. *Journal*
577 *of Vegetation Science*, **24**, 794–806.
- 578 Mason, N.W.H., Lanoiselée, C., Mouillot, D., Wilson, J.B. & Argillier, C. (2008). Does niche overlap
579 control relative abundance in French lacustrine fish communities? A new method
580 incorporating functional traits. *Journal of Animal Ecology*, **77**, 661–669.
- 581 Mason, N.W.H., Mouillot, D., Lee, W.G. & Wilson, J.B. (2005). Functional richness, functional
582 evenness and functional divergence: the primary components of functional diversity. *Oikos*,
583 **111**, 112–118.
- 584 Mason, N.W.H. & Wilson, J.B. (2006). Mechanisms of species coexistence in a lawn community:
585 mutual corroboration between two independent assembly rules. *Community Ecology*, **7**,
586 109–116.
- 587 Mayfield, M.M. & Levine, J.M. (2010). Opposing effects of competitive exclusion on the phylogenetic
588 structure of communities. *Ecology Letters*, **13**, 1085–1093.
- 589 Meszéna, G., Gyllenberg, M., Pásztor, L. & Metz, J.A.J. (2006). Competitive exclusion and limiting
590 similarity: A unified theory. *Theoretical Population Biology*, **69**, 68–87.
- 591 Montaña, C.G., Winemiller, K.O. & Sutton, A. (2014). Intercontinental comparison of fish
592 ecomorphology: null model tests of community assembly at the patch scale in rivers.
593 *Ecological Monographs*, **84**, 91–107.
- 594 Mouchet, M.A., Villéger, S., Mason, N.W.H. & Mouillot, D. (2010). Functional diversity measures: an
595 overview of their redundancy and their ability to discriminate community assembly rules.
596 *Functional Ecology*, **24**, 867–876.
- 597 Mouillot, D., Dumay, O. & Tomasini, J.A. (2007). Limiting similarity, niche filtering and functional
598 diversity in coastal lagoon fish communities. *Estuarine, Coastal and Shelf Science*, **71**, 443–
599 456.
- 600 Münkemüller, T., de Bello, F., Meynard, C.N., Gravel, D., Lavergne, S., Mouillot, D., Mouquet, N. &
601 Thuiller, W. (2012). From diversity indices to community assembly processes: a test with
602 simulated data. *Ecography*, **35**, 468–480.
- 603 Pakeman, R., Lennon, J. & Brooker, R. (2011). Trait assembly in plant assemblages and its modulation
604 by productivity and disturbance. *Oecologia*, **167**, 209–218.
- 605 Pärtel, M., Szava-Kovats, R. & Zobel, M. (2011). Dark diversity: shedding light on absent species.
606 *Trends in Ecology & Evolution*, **26**, 124–128.
- 607 Pavoine, S. & Bonsall, M.B. (2011). Measuring biodiversity to explain community assembly: a unified
608 approach. *Biological Reviews*, **86**, 792–812.
- 609 Pillar, V.D., Duarte, L. da S., Sosinski, E.E. & Joner, F. (2009). Discriminating trait-convergence and
610 trait-divergence assembly patterns in ecological community gradients. *Journal of Vegetation*
611 *Science*, **20**, 334–348.

- 612 Podani, J. (2009). Convex hulls, habitat filtering, and functional diversity: mathematical elegance
613 versus ecological interpretability. *Community Ecology*, **10**, 244–250.
- 614 Raavel, V., Violle, C. & Munoz, F. (2012). Mechanisms of ecological succession: insights from plant
615 functional strategies. *Oikos*, **121**, 1761–1770.
- 616 Rosindell, J., Hubbell, S.P., He, F., Harmon, L.J. & Etienne, R.S. (2012). The case for ecological neutral
617 theory. *Trends in Ecology & Evolution*, **27**, 203–208.
- 618 Shipley, B. (2014). Measuring and interpreting trait-based selection versus meta-community effects
619 during local community assembly. *Journal of Vegetation Science*, **25**, 55–65.
- 620 Shipley, B., Paine, C.E.T. & Baraloto, C. (2012). Quantifying the importance of local niche-based and
621 stochastic processes to tropical tree community assembly. *Ecology*, **93**, 760–769.
- 622 Spasojevic, M.J. & Suding, K.N. (2012). Inferring community assembly mechanisms from functional
623 diversity patterns: the importance of multiple assembly processes. *Journal of Ecology*, **100**,
624 652–661.
- 625 Stubbs, W.J. & Wilson, J.B. (2004). Evidence for limiting similarity in a sand dune community. *Journal*
626 *of Ecology*, **92**, 557–567.
- 627 Swenson, N.G., Enquist, B.J., Pither, J., Thompson, J. & Zimmerman, J.K. (2006). The problem and
628 promise of scale dependency in community phylogenetics. *Ecology*, **87**, 2418–2424.
- 629 Vamosi, S.M., Heard, S.B., Vamosi, J.C. & Webb, C.O. (2009). Emerging patterns in the comparative
630 analysis of phylogenetic community structure. *Molecular Ecology*, **18**, 572–592.
- 631 Vellend, M., Srivastava, D.S., Anderson, K.M., Brown, C.D., Jankowski, J.E., Kleynhans, E.J., Kraft,
632 N.J.B., Letaw, A.D., Macdonald, A.A.M., Maclean, J.E., Myers-Smith, I.H., Norris, A.R. & Xue, X.
633 (2014). Assessing the relative importance of neutral stochasticity in ecological communities.
634 *Oikos*, **123**, 1420–1430.
- 635 Villéger, S., Mason, N.W.H. & Mouillot, D. (2008). New multidimensional functional diversity indices
636 for a multifaceted framework in functional ecology. *Ecology*, **89**, 2290–2301.
- 637 Weiher, E., Clarke, G.D.P. & Keddy, P.A. (1998). Community Assembly Rules, Morphological
638 Dispersion, and the Coexistence of Plant Species. *Oikos*, **81**, 309–322.
- 639 Weiher, E., Freund, D., Bunton, T., Stefanski, A., Lee, T. & Bentivenga, S. (2011). Advances, challenges
640 and a developing synthesis of ecological community assembly theory. *Philosophical*
641 *Transactions of the Royal Society B: Biological Sciences*, **366**, 2403–2413.
- 642 Willis, C.G., Halina, M., Lehman, C., Reich, P.B., Keen, A., McCarthy, S. & Cavender-Bares, J. (2010).
643 Phylogenetic community structure in Minnesota oak savanna is influenced by spatial extent
644 and environmental variation. *Ecography*, **33**, 565–577.
- 645 Wilson, J.B. (2011). The twelve theories of co-existence in plant communities: the doubtful, the
646 important and the unexplored. *Journal of Vegetation Science*, **22**, 184–195.
- 647
- 648

650 Table 1: Parameters of the individual based simulation and the values used in the sensitivity analysis

Name	Description	Step	Values explored	Remark
S	number of species in the regional species pool	all	200, 133, 300	
N	number of local communities	all	50, 33, 75	
J	number of individuals in a local community	all	300, 200, 450	
d	parameter of the symmetric beta distribution used for generating trait values	1	1, 0.5, 1.5	these values give uniform (d=1), arcsine (0.5), and Wigner semicircle distributions (1.5)
c	parameter for setting the correlation between traits A and B	1	0, -6, 0.6	see equation (1) in Appendix S2, at c = 0 there is no correlation, whereas c = ± 6 means a correlation of $\sim \pm .83$
R	the fraction of the environmental gradient covered by the local communities	1	0.8, 0.6, 0.9	
σ_A	tolerance width	1, 5	0.05, 0.01, 0.25, ∞	determines habitat filtering, with lower values meaning more specialist species (see equation 2 and figure S2.1 in Appendix S2). At $\sigma_A = \infty$ species are maximally generalist (abiotic conditions do not influence their abundance).
σ_B	scaling parameter of the competition strength	3	0.05, 0.01, 0.25, 0	determines limiting similarity, with higher values meaning stronger competition (see equations 4 and 5 and figure S2.1 in Appendix S2) At $\sigma_B = 0$ there is no interspecific competition (no effect of trait B on competition).
b	probability of reproduction at no competition	3	1	see equation (3) in Appendix S2
K_0	critical level of competitive pressure	3	200, 133, 300	see equation (3) in Appendix S2
m	probability of dispersing seeds to another local community	4	0.1, 0.066, 0.15	the target community is selected randomly (without regard to spatial location or closeness)

sim.len the length of the
simulation

100, 66, 150

the total number of iterations is
 $\text{sim.len} * J$

651 Table 2: Overview of the tested functional diversity indices

Name	Description	Measured component ¹	Abundances used?	References
FRic	Convex hull volume (or range in the one-dimensional case)	functional richness	No	(Cornwell <i>et al.</i> 2006; Villéger <i>et al.</i> 2008)
RaoQ	Rao's quadratic entropy (=Mean distance among species weighted by species abundance)	functional richness and divergence	Yes	(Botta-Dukát 2005)
FEve	Evenness in the branch lengths of a minimum spanning tree	functional evenness	Yes	(Villéger <i>et al.</i> 2008)
Vd	Variance of distances	functional evenness	No	(Clarke & Warwick 2001)
Vnnd	Variance in the nearest-neighbor distances	functional evenness	No	(Weiher <i>et al.</i> 1998)

652

653 ¹ sensu Laliberte & Legendre 2010

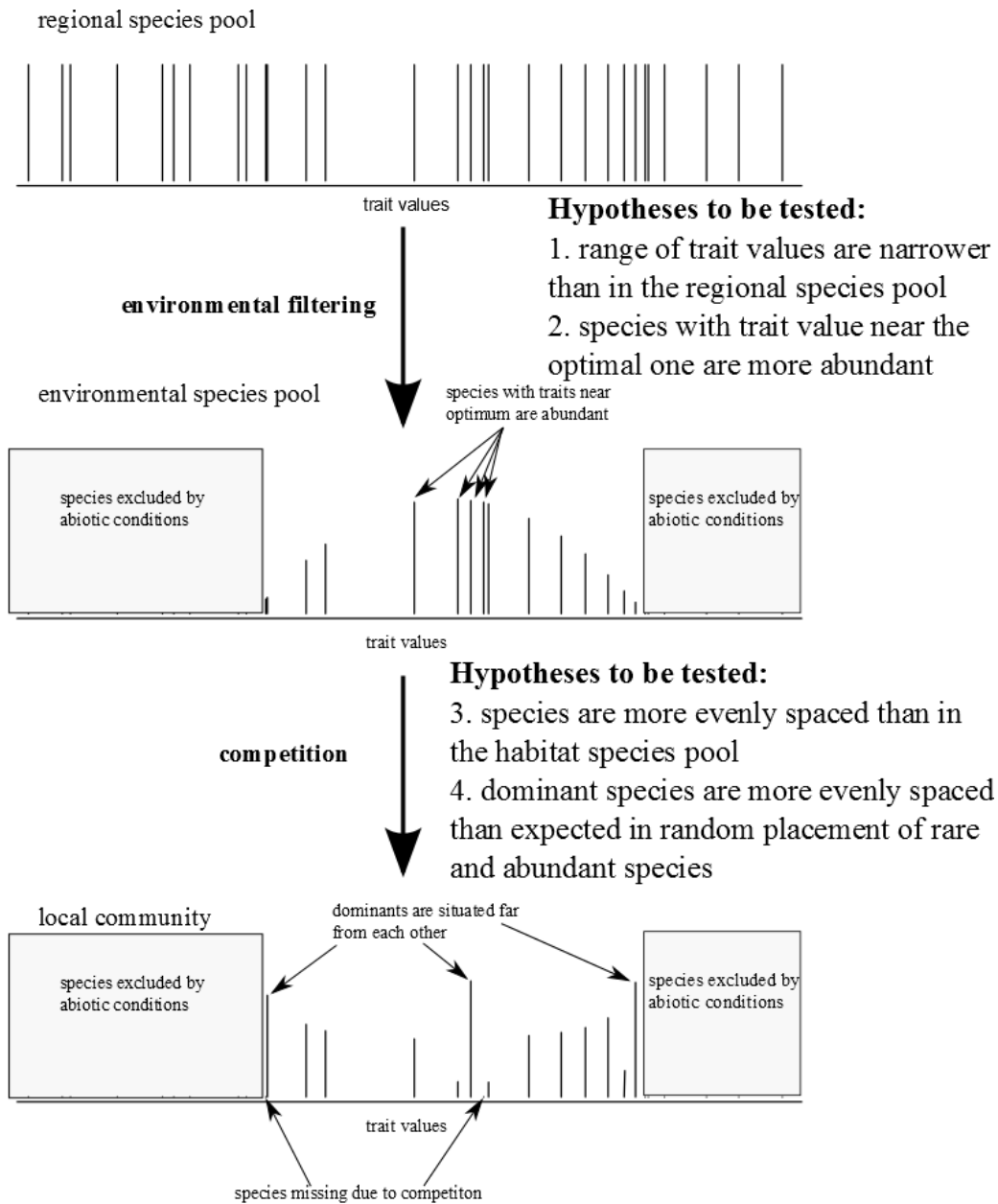
654

655 **Table 3:** Overview of the alternative hypotheses applied. For calculating type I error rate both habitat
 656 filtering and limiting similarity were switched off by appropriate parameter settings or using neutral
 657 trait. For testing power, only the trait expected to converge/diverge was used in the calculations.

Randomization	test statistic	Power for detecting convergence	Power for detecting divergence	Type I error rate
Between-plot	FRic	one sided observed<random	one sided observed>random	two sided
	RaoQ			
	FEve			
	Vd	one sided observed>random	one sided observed<random	
Within-plot	Vnnd	not applied	one sided observed>random	one sided observed>random
	RaoQ	not applied	one sided observed>random	one sided observed>random
FEve	one sided observed>random		one sided observed>random	
Restricted	FRic		one sided observed>random	one sided observed>random
	RaoQ		one sided observed<random	one sided observed<random
	FEve		one sided observed<random	one sided observed<random
	Vd			
	Vnnd			

658

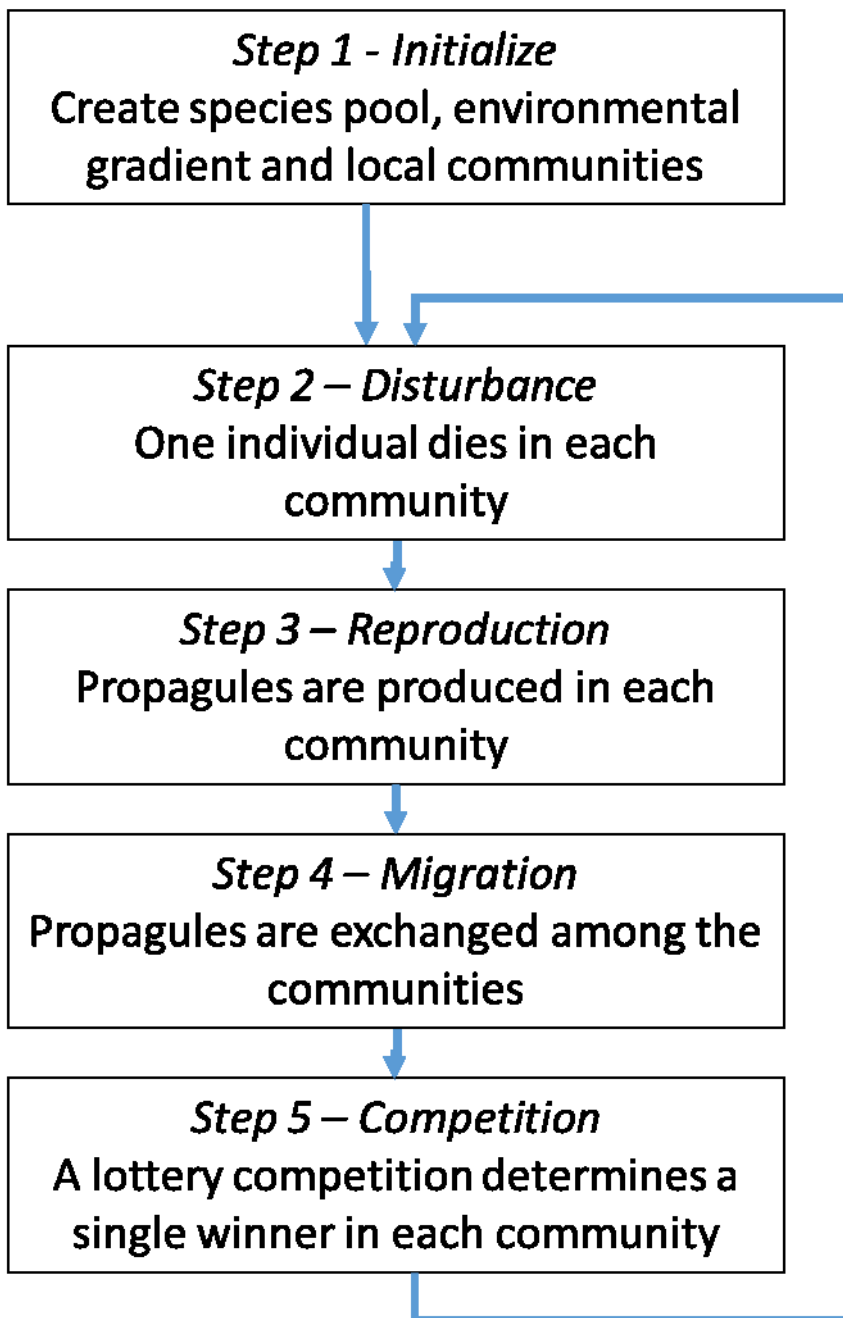
659



660

661 Figure 1: Expected changes in the distribution of trait values due to habitat filtering and competition,
 662 and the related hypotheses to be tested. Since the regional and the environmental species pool are
 663 often not known, they are substituted by the pool of observed species (in the between-plot
 664 randomization strategy) or occurring just in the local plot (in the within-plot strategy).

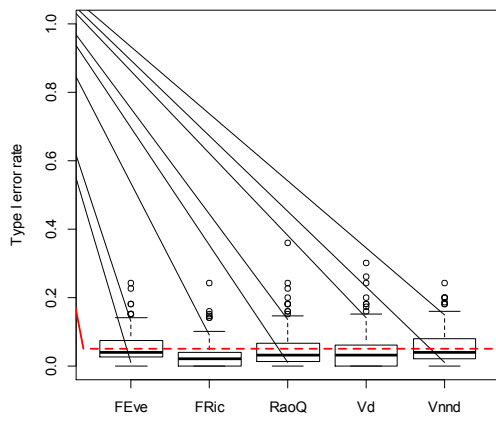
665



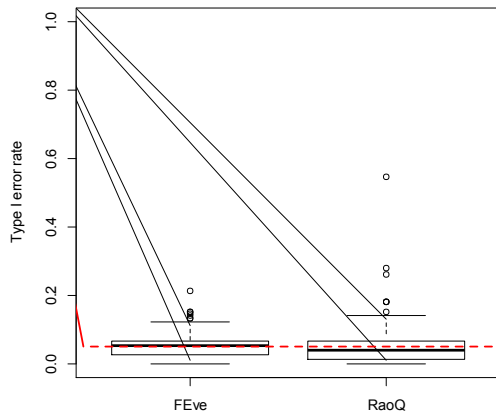
666

667 Figure 2: Flow-chart of the individual based simulation.

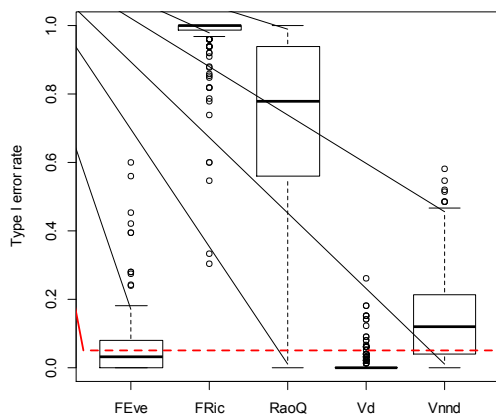
668



669
670 a)



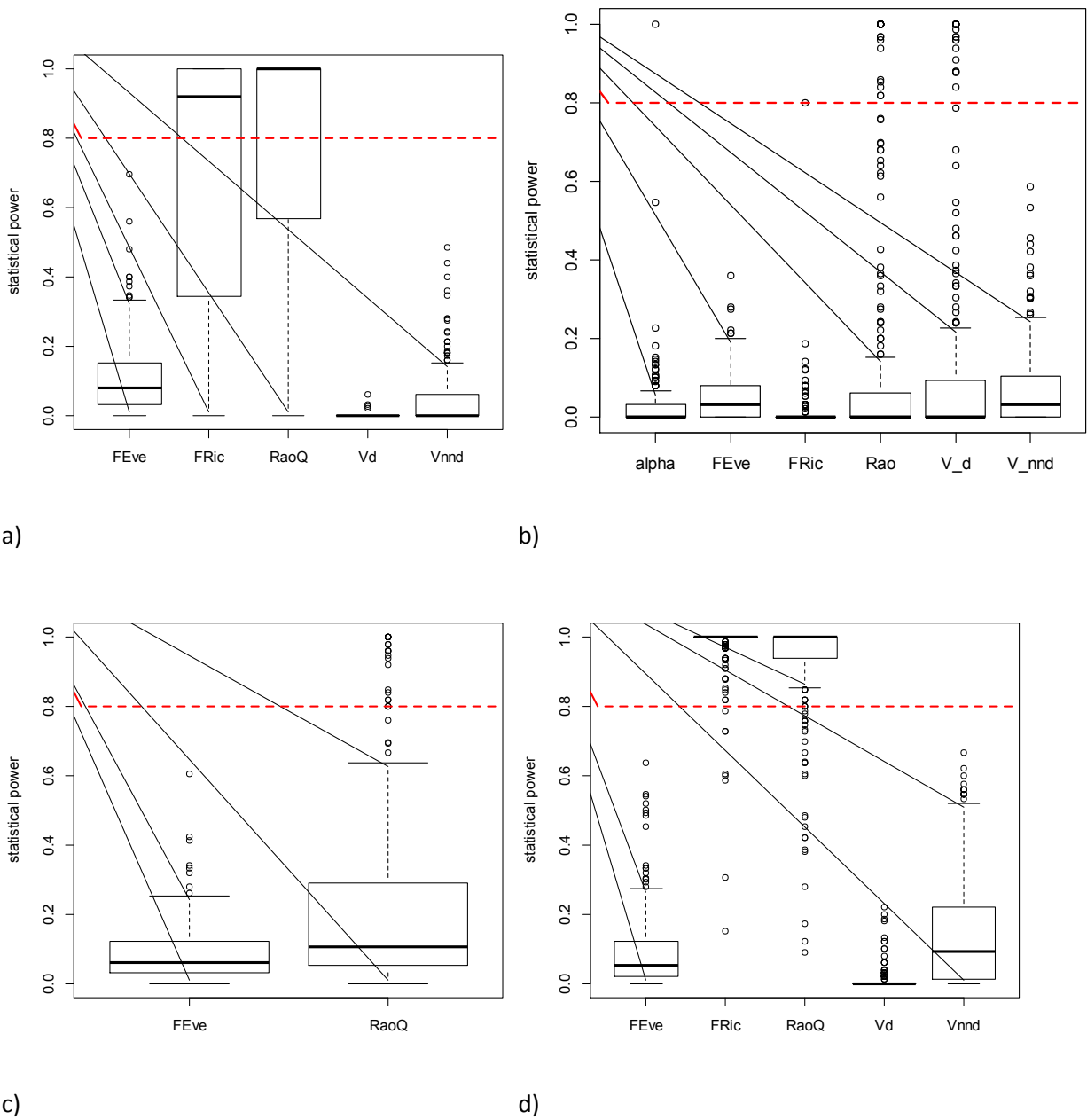
671
672 b)



673
674 c)

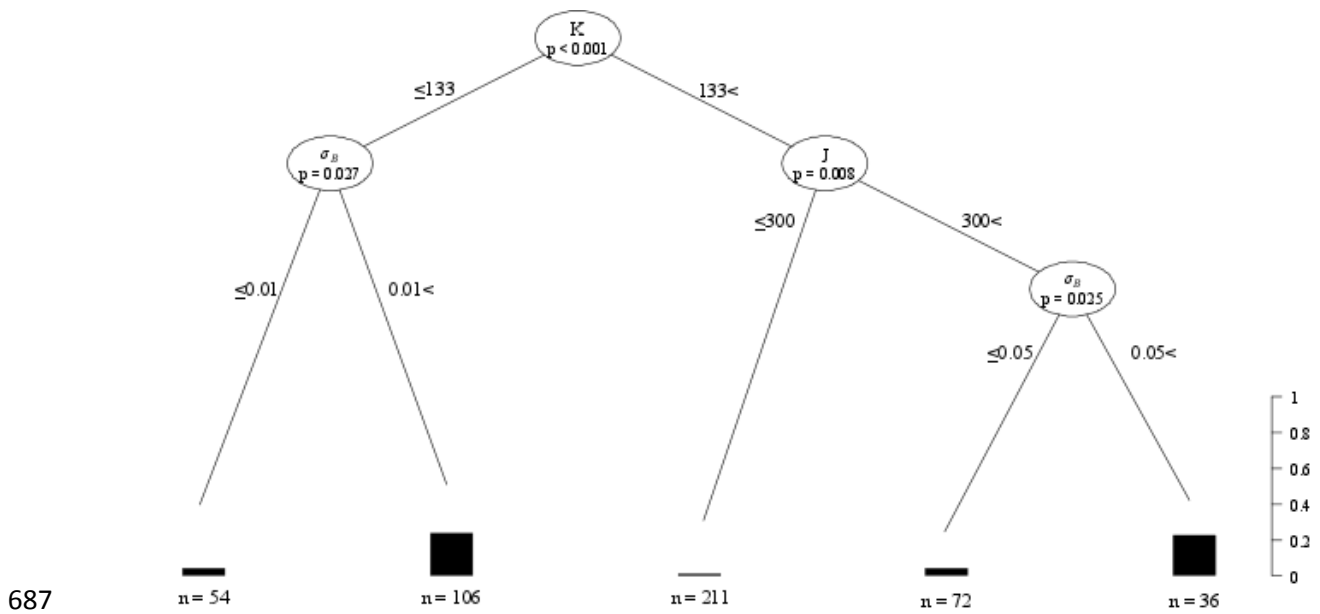
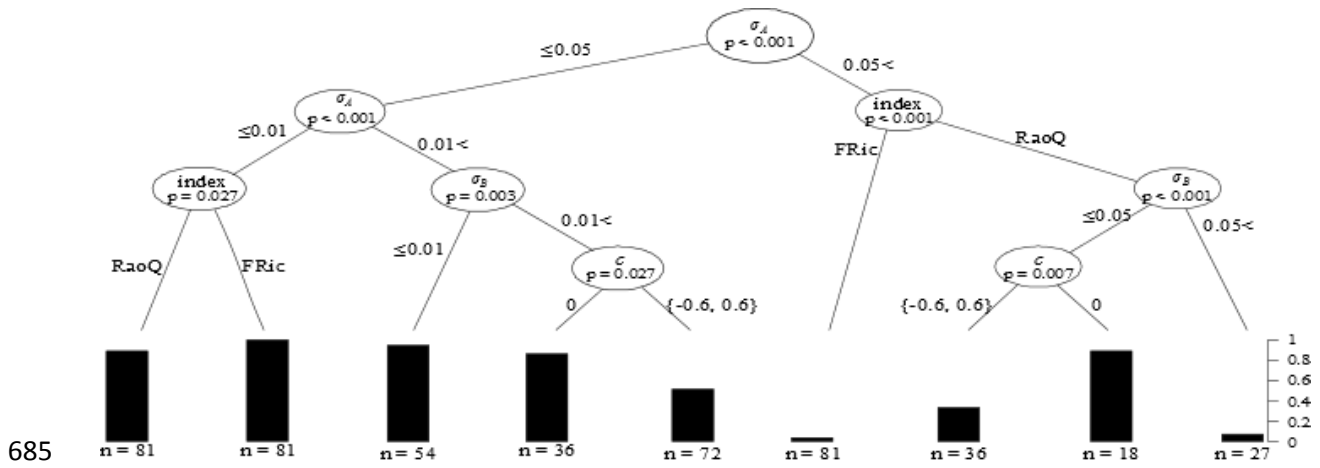
675 **Figure 3: Boxplots of the type I error rates in between-plot (a), within-plot(b) and restricted randomization (c) estimated**
676 **by using neutral traits . Dashed red line indicates the pre-defined significance level (i.e. 5%).**

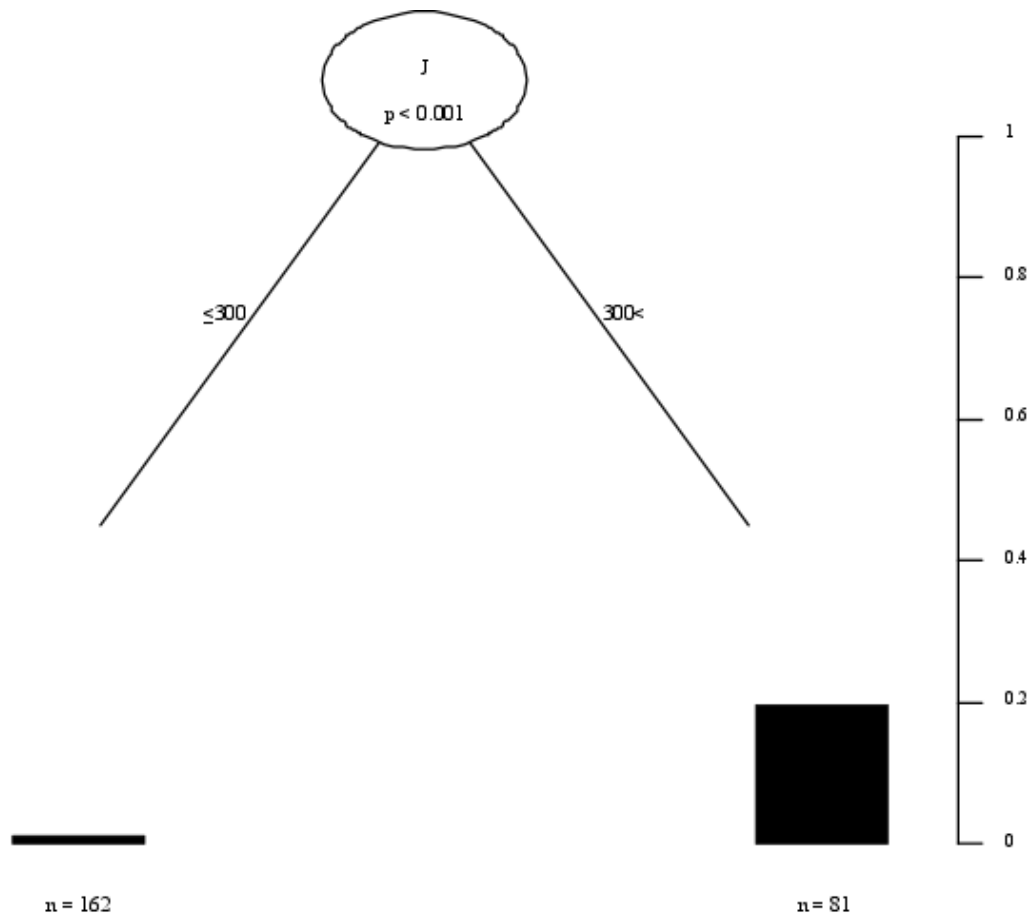
677
678



679
680
681
682
683
684

Figure 4: The power of the tests applying different indices. Dashed line indicates a threshold above which the statistical power of the test is generally accepted. (a) detecting trait convergence by using the between-plot randomization strategy, (b) detecting trait divergence by using the between-plot randomization strategy, (c) detecting trait divergence by using the within-plot randomization strategy, (d) detecting trait divergence by using the restricted randomization strategy





689

690 c)

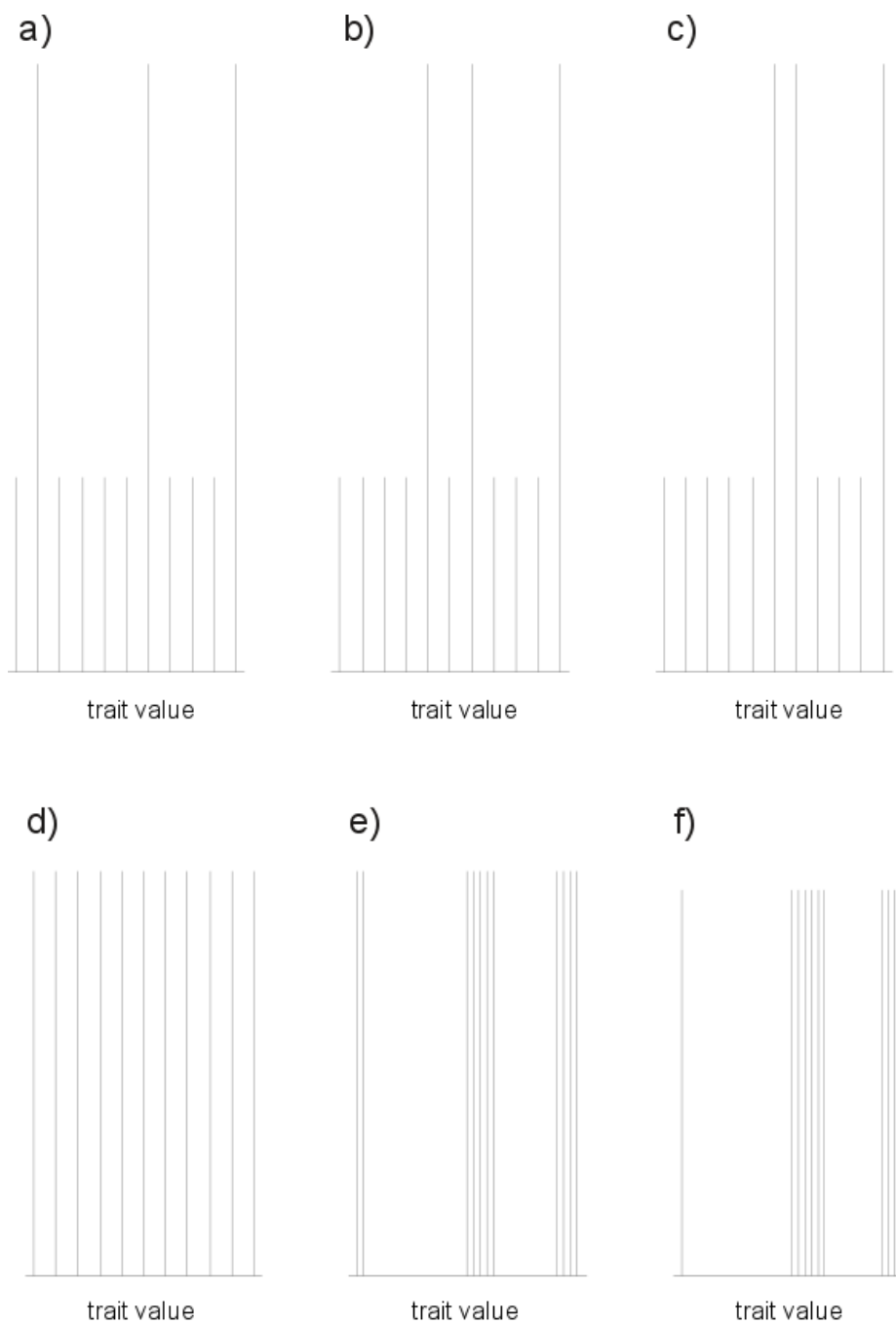
691 **Figure 5: Classification tree models for revealing the effect of parameters and indicator choice on the power of tests.**
 692 **Each internal node describes a statistically significant split (with splitting variable and p value given in the node, and split**
 693 **values given on the branches below), whereas terminal nodes give the number of complying cases (n) and a visual**
 694 **summary of the response variable (rate of cases above the 0.8 threshold). (a) trait convergence tests using between-plot**
 695 **randomization. Only FRic and RaoQ were involved into this analysis. (b) trait divergence tests using between-plot**
 696 **randomization Only RaoQ and Vd were involved into this analysis. (c) trait divergence tests using within-plot**
 697 **randomization Only RaoQ was involved into this analysis**

698

699

700

701



702

703

704

705

706

707

708

709

710

Figure 6: Hypothetical communities for illustrating that both FEve (a-c) and variance of nearest neighbor distance (Vnnd) (d-f) failed to correctly measure the functional evenness because they consider only the (nearest) neighbor species. Each vertical line represents a trait value of the species, while height shows the abundance. FEve is the same for community a) and b), while lower in c). Vnnd is zero in both communities d) and e), but high in community f). These examples illustrate the unfavorable property of these indices that considerably different communities may results in the same value of the index, while in other cases small community changes may cause major changes in the index values. Furthermore, pattern in communities a) and d) may be caused by limiting similarity, while the other patterns contradict this theory, but the values of the indices do not show this difference. Note that communities a-c differ only in position of

711 abundant and rare species, thus they can be considered as illustrations of a within-plot randomization strategy: if
712 community a) is the field data, the same low values can be easily obtained during the randomization.

713

714 **Appendix S1:** Illustrative examples of the diversity of test statistics used for testing trait
 715 divergence/convergence in field case studies

Test statistic	Used for testing		
	trait convergence	trait divergence	both convergence and divergence
FRic	Cornwell <i>et al.</i> 2006; Kraft <i>et al.</i> 2008; Cornwell & Ackerly 2009; Bernard-Verdier <i>et al.</i> 2012; Raavel <i>et al.</i> 2012; Yan <i>et al.</i> 2012		Schamp <i>et al.</i> 2008; Schamp & Aarssen 2009
Vnnd ¹		Cornwell & Ackerly 2009; Schamp & Aarssen 2009; Yan <i>et al.</i> 2012; Montaña <i>et al.</i> 2013	Schamp <i>et al.</i> 2008
RaoQ ²		Mason & Wilson 2006; Bernard-Verdier <i>et al.</i> 2012	Smith <i>et al.</i> 1994; Schamp <i>et al.</i> 2008; de Bello <i>et al.</i> 2009; Thompson <i>et al.</i> 2010; Paillex <i>et al.</i> 2013
FEve		Raavel <i>et al.</i> 2012	

716 ¹ includes both the variance and the standard deviation of nearest neighbor distances

717 ² If only one trait is considered and Euclidean distance is applied, RaoQ is a weighted variance of trait
 718 values. Therefore case studies using variance of trait values are listed here.

719

720 De Bello, F., Thuiller, W., Lepš, J., Choler, P., Clément, J.-C., Macek, P., Sebastià, M.-T. & Lavorel, S.
 721 (2009). Partitioning of functional diversity reveals the scale and extent of trait convergence
 722 and divergence. *Journal of Vegetation Science*, **20**, 475–486.

723 Bernard-Verdier, M., Navas, M.-L., Vellend, M., Violle, C., Fayolle, A. & Garnier, E. (2012). Community
 724 assembly along a soil depth gradient: contrasting patterns of plant trait convergence and
 725 divergence in a Mediterranean rangeland. *Journal of Ecology*, **100**, 1422–1433.

726 Cornwell, W.K. & Ackerly, D.D. (2009). Community assembly and shifts in plant trait distributions
 727 across an environmental gradient in coastal California. *Ecological Monographs*, **79**, 109–126.

728 Cornwell, W.K., Schwilk, D.W. & Ackerly, D.D. (2006). A trait-based test for habitat filtering: convex
 729 hull volume. *Ecology*, **87**, 1465–1471.

730 Kraft, N.J.B., Valencia, R. & Ackerly, D.D. (2008). Functional Traits and Niche-Based Tree Community
 731 Assembly in an Amazonian Forest. *Science*, **322**, 580–582.

732 Laliberté, E. & Legendre, P. (2010). A distance-based framework for measuring functional diversity
 733 from multiple traits. *Ecology*, **91**, 299–305.

- 734 Mason, N.W.H. & Wilson, J.B. (2006). Mechanisms of species coexistence in a lawn community:
735 mutual corroboration between two independent assembly rules. *Community Ecology*, **7**,
736 109–116.
- 737 Montaña, C.G., Winemiller, K.O. & Sutton, A. (2014). Intercontinental comparison of fish
738 ecomorphology: null model tests of community assembly at the patch scale in rivers.
739 *Ecological Monographs*, **84**, 91–107
- 740 Paillex, A., Doledec, S., Castella, E., Merigoux, S. & Aldridge, D.C. (2013). Functional diversity in a large
741 river floodplain: anticipating the response of native and alien macroinvertebrates to the
742 restoration of hydrological connectivity. *Journal of Applied Ecology*, **50**, 97–106.
- 743 Raavel, V., Violle, C. & Munoz, F. (2012). Mechanisms of ecological succession: insights from plant
744 functional strategies. *Oikos*, **121**, 1761–1770.
- 745 Schamp, B.S. & Aarssen, L.W. (2009). The assembly of forest communities according to maximum
746 species height along resource and disturbance gradients. *Oikos*, **118**, 564–572.
- 747 Schamp, B.S., Chau, J. & Aarssen, L.W. (2008). Dispersion of traits related to competitive ability in an
748 old-field plant community. *Journal of Ecology*, **96**, 204–212.
- 749 Smith, B., Moore, S.H., Grove, P.B., Harris, N.S., Mann, S. & Wilson, J.B. (1994). Vegetation texture as
750 an approach to community structure - community-level convergence in a New-Zealand
751 temperate rain-forest. *New Zealand Journal of Ecology*, **18**, 41–50.
- 752 Thompson, K., Petchey, O.L., Askew, A.P., Dunnett, N.P., Beckerman, A.P. & Willis, A.J. (2010). Little
753 evidence for limiting similarity in a long-term study of a roadside plant community. *Journal of*
754 *Ecology*, **98**, 480–487.
- 755 Yan, B., Zhang, J., Liu, Y., Li, Z., Huang, X., Yang, W. & Prinzing, A. (2012). Trait assembly of woody
756 plants in communities across sub-alpine gradients: Identifying the role of limiting similarity.
757 *Journal of Vegetation Science*, **23**, 698–708.
- 758
- 759

760 **Appendix S2:** Detailed description of the simulation model applied

761

762 The main steps

763 **Step 1:** A regional species pool consisting of S species is created. Each species is characterized by
764 three numeric traits (A, B and C). Trait A is related to habitat matching, trait B regulates resource
765 acquisition, while trait C is neutral. Trait values, which always range between 0 and 1, are sampled
766 from the same prespecified symmetric beta distribution (uniform, arcsine or Wigner semicircle
767 distribution). Correlations between traits A and B are added with the help of a correlation parameter
768 (c) in the following way:

769
$$A = c S_B + (1 - c) S_A, \text{ and } B = c S_A + (1 - c) S_B \quad \text{if } c \geq 0, \text{ and}$$

770
$$A = |c| (1 - S_B) + (1 - |c|) S_A, \text{ and } B = |c| (1 - S_A) + (1 - |c|) S_B \quad \text{if } c \leq 0 \quad (1)$$

771 where S_A and S_B are the random variables from the specified beta distribution, and A and B are the
772 trait values.

773 To initialize the environmental gradient, n local communities get positioned equidistantly along a
774 pre-specified central part of the range of trait A. As the position of the local communities along the
775 gradient actually determines the optimal value of trait A for each community, the position is
776 characterized by this “optimal trait value” itself, rather than any arbitrarily defined artificial
777 environmental data.

778 In the last part of the initialization process, the local communities get filled up with species from the
779 species pool until the predefined total number of individuals (J) is reached. J is set to be equal for all
780 of the communities. Propagules are assumed to arrive from the species pool at the same rate for all
781 species, while their survival is considered to depend on the suitability of the local conditions for the
782 species. Accordingly, the initial communities are constructed as a random sample of size J from the
783 species pool with the survival probabilities (s_{jk}) for species i in local community k calculated in the
784 following way (Gaussian survival functions):

785
$$s_{ik} = \exp\left(-\frac{(A_k - A_i)^2}{2\sigma_A^2}\right) \quad (2)$$

786 where: A_k is the position of community k along the environmental gradient (i.e. the local optimum for
 787 trait A), A_i is the value of trait A for species i , and σ_A is the parameter determining the tolerance
 788 width of the species (considered to be constant for all species). The influence of σ_A on the outcome
 789 of a lottery competition for local adaptedness between two species is illustrated in Figure S2.1.

790 **Step 2:** In each local community a single individual dies in this step. To keep the simulation as simple
 791 as possible, each individual has the same probability for being selected, irrespective of their traits or
 792 their “age”.

793 **Step 3:** Each individual produces zero or one seed in this step. The probability of reproduction of
 794 species i in local community k depends on the competition for resources:

795
$$p_{ik} = b \max\left(\frac{K_0 - K_{ik}}{K_0}, 0\right) \quad (3)$$

796 where K_{ik} is the competitive pressure for species i in community j , K_0 is the critical level of
 797 competitive pressure above which the probability of reproduction becomes zero, and b is the
 798 background reproduction probability at no competition (considered to be equal for all species). The
 799 competitive pressure is determined as:

800
$$K_{ik} = \sum_j n_{jk} C_{ij} \quad (4)$$

801 where C_{ij} is the level of competition between species i and j , and n_{jk} is the abundance of species j in
 802 the local community (k). The level of competition between two species depends on their similarity in
 803 trait B (the resource acquisition trait):

804
$$C_{ij} = \exp\left(-\frac{(B_i - B_j)^2}{\sigma_B}\right) \quad (5)$$

805 where σ_B is a scaling parameter for setting the strength of interspecific competition, set to be the
 806 same for each pair of species. The maximum value of C_{ij} is thus 1 (if $i = j$, i.e. intraspecific

807 competition), while the minimum value possible over the whole range of B values (i.e. from 0 to 1) is
808 set by σ_B as:

$$809 \quad C_{min} = \exp\left(-\frac{1}{\sigma_B}\right) \quad (6)$$

810 The effect of σ_B on the strength of competition for resources between two species is illustrated in
811 Figure S2.2.

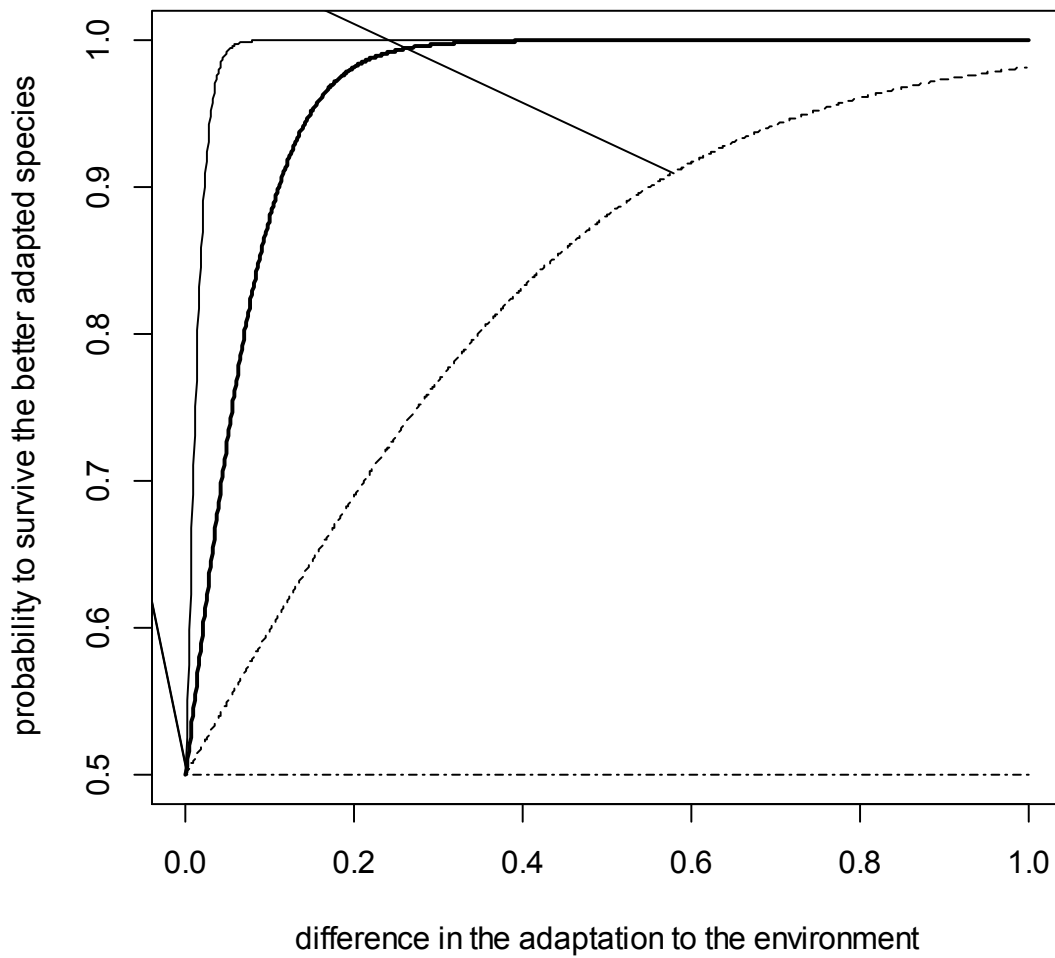
812 **Step 4:** To simulate simple metapopulation dynamics, each seed produced can spread to one of the
813 other local communities with probability m . Nevertheless, the target locality is chosen randomly
814 without considering any “spatial position” for the local communities.

815 **Step 5:** In this last step, a lottery competition¹ takes place among the seedlings germinating from the
816 seeds produced locally or having arrived from the other localities in the previous step. This is set to
817 be a stochastic process with the probability of winning being proportional to s_{ik} (equation (2)) for the
818 seedlings of species i at location k , thus not necessary the best adapted species will win (Figure S2.1).
819 In each turn only one seedling can survive, all other propagules are lost. This surviving seedling
820 matures by the next iteration, and become a fully functional individual capable of reproduction in full
821 competition with all other individuals of the local community.

822 **Iteration cycles:** After having completed step 1 once, steps 2-5 are repeated many times for each
823 local community so that the final composition is independent from the colonization process. Since
824 changes are slower at larger community sizes, the number of cycles was set to 60-150 times (*sim.len*,
825 see Table 1) the number of individuals in a local community (J). The “convergence” of this iterative
826 process is illustrated in Figures S2.3-5 with the help of a randomly selected simulation run.

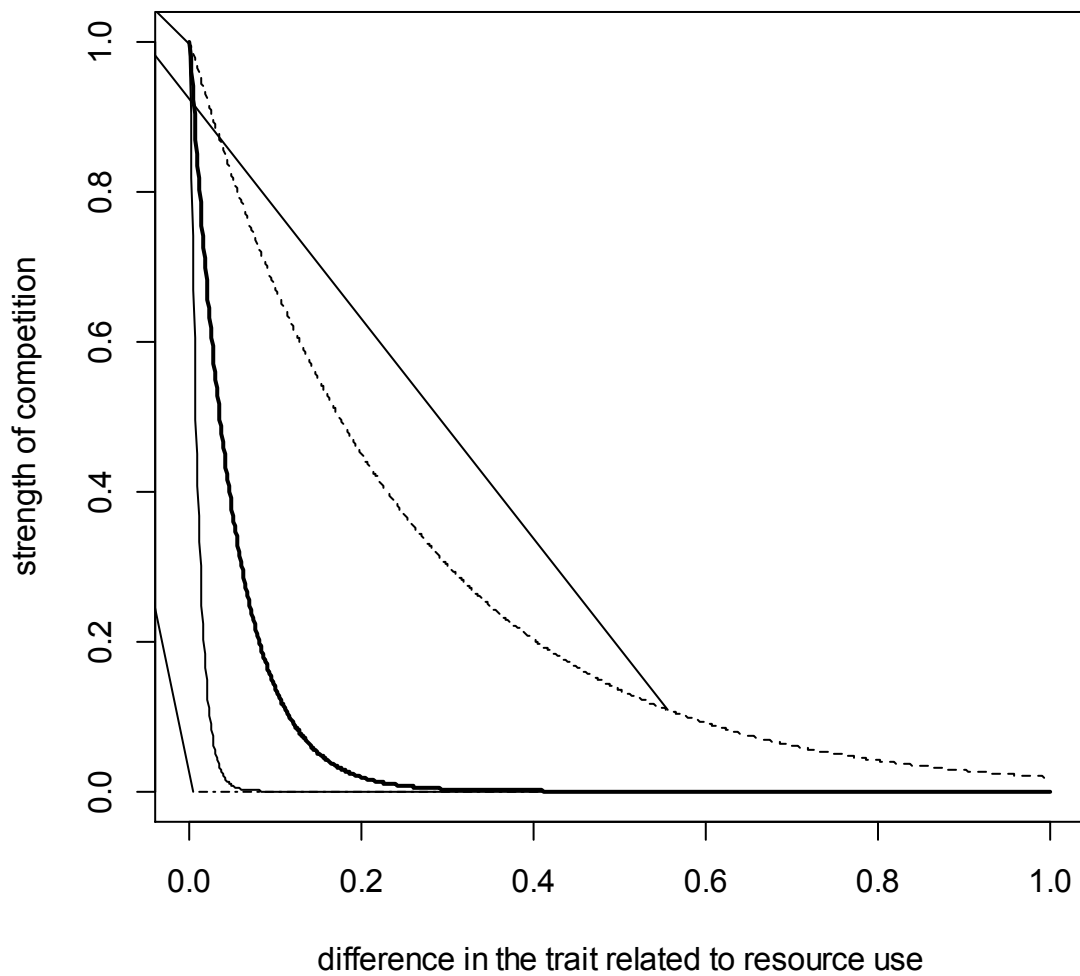
827

¹Chesson, P.L. & Warner, R.R. (1981). Environmental Variability Promotes Coexistence in Lottery Competitive Systems. *The American Naturalist*, **117**, 923–943.



828

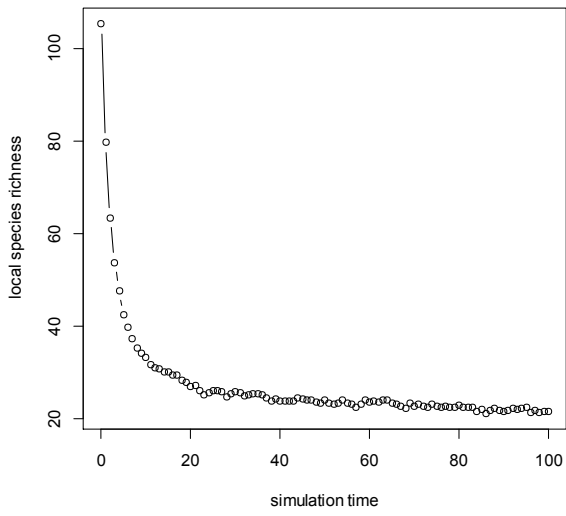
829 **Figure S2.1.** The effect of σ_A governing habitat filtering on the outcome of a lottery competition
 830 between two species for local adaptedness. The four lines shown correspond to the values tested in
 831 this study: $\sigma_A = 0.01$ (thin solid line); $\sigma_A = 0.05$ (thick solid line); $\sigma_A = 0.25$ (dashed line) and $\sigma_A = \infty$
 832 (dashed-dotted line).



833

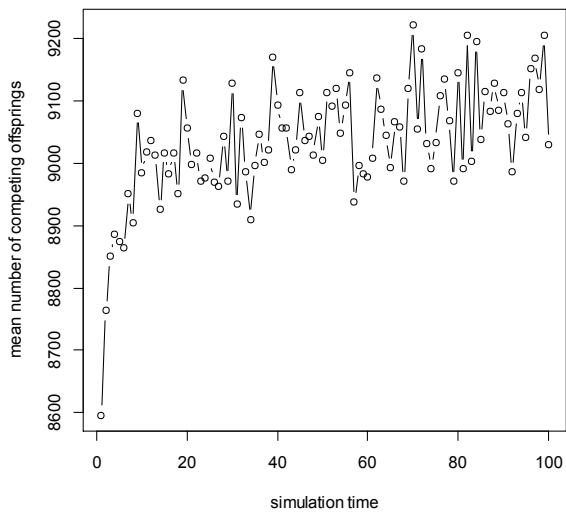
834 **Figure S2.1.** The effect of σ_B on the strength of competition for resources between two species in
 835 the simulation model. The four lines shown correspond to the values tested in this study: $\sigma_B = 0.01$
 836 (thin solid line); $\sigma_B = 0.05$ (thick solid line); $\sigma_B = 0.25$ (dashed line); and $\sigma_B = 0$ (dashed-dotted line).

837



838

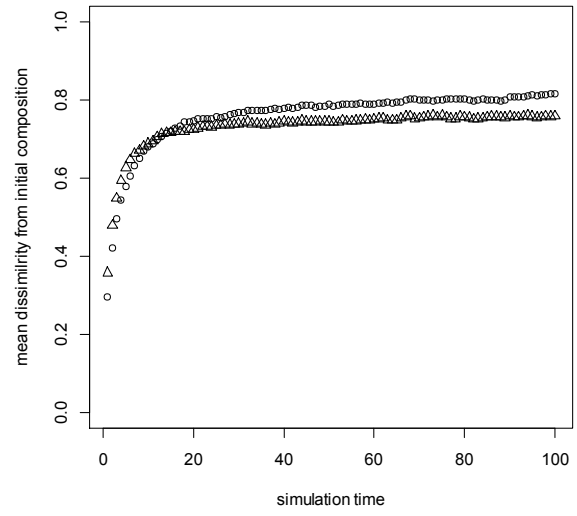
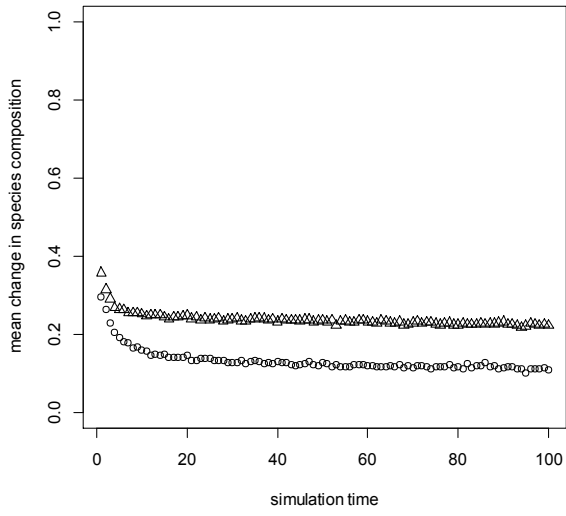
839 **Figure S2.3:** Typical change in local species richness (the mean number of species in each local
 840 community) during a simulation run



841

842 **Figure S2.4.** Changes in the mean number of competing seedlings during a simulation. Note that only
 843 one of them can grow up, all others die.

844



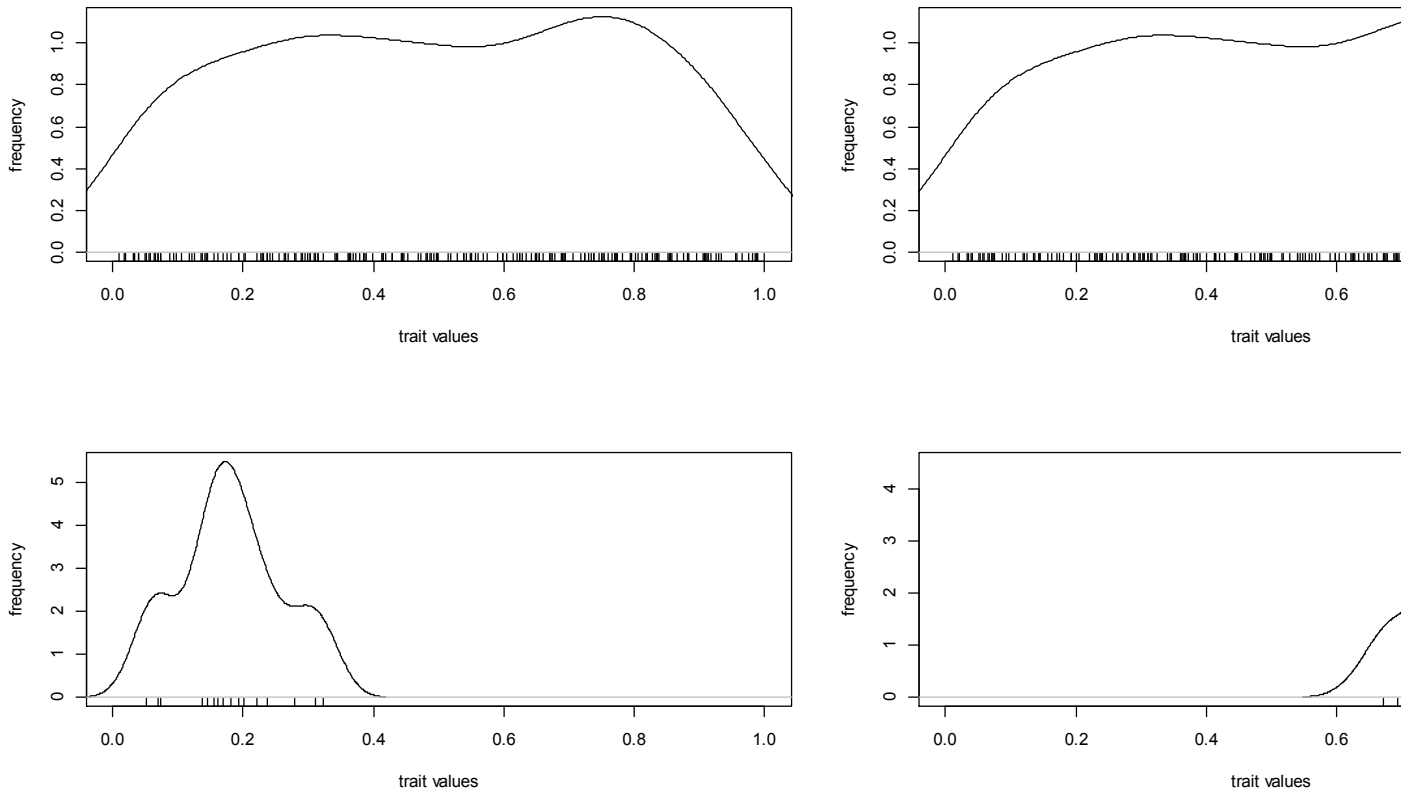
a)

b)

845 **Figure S2.5.** Changes in species composition decrease during the simulation. (a) Mean Bray-Curtis
 846 dissimilarity between consecutive steps. (b) Mean Bray-Curtis dissimilarity from the starting
 847 composition. Circles: simulation with baseline parameter values, triangles: neutral dynamics with
 848 baseline parameter values.

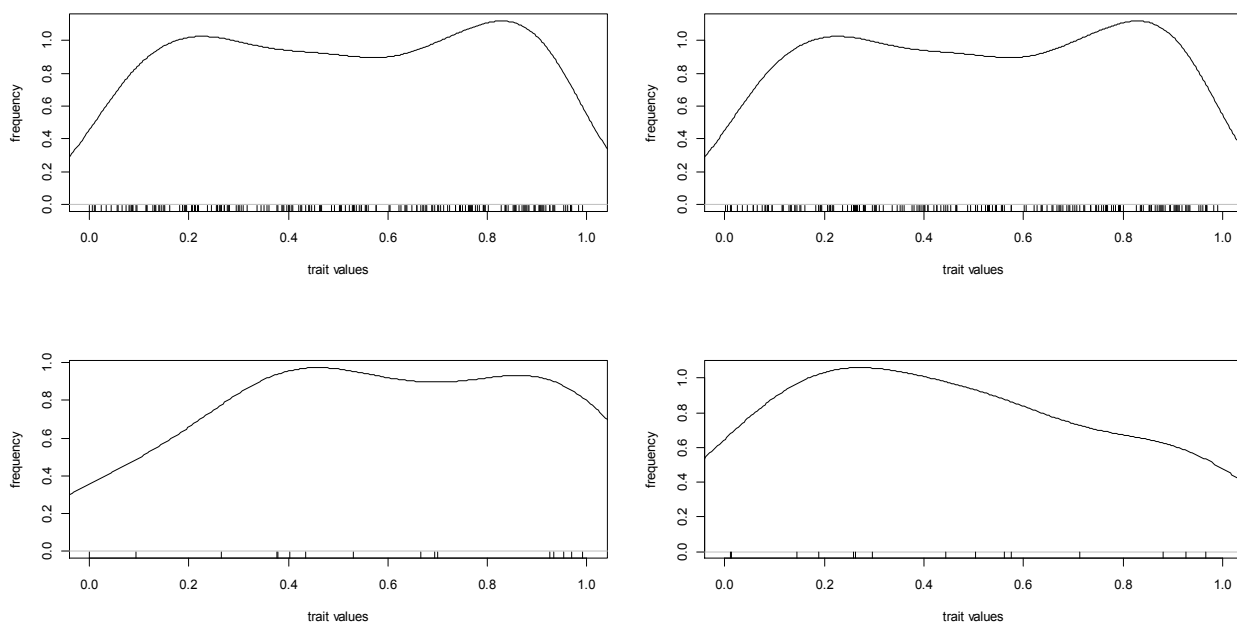
849

850 **Appendix S3:** Comparison of trait distribution in the initial regional species pool, in the pool of
851 observed species, and two local communities



852

853 Figure S3.1 Distribution of trait A (related to environmental tolerance) in the initial regional species
854 pool (a), and three set of species pools after a simulation run with baseline values: trait values in the
855 pool of observed species (b), and species occurring in the first (c) and last local community (d) along
856 the environmental gradient. The line is a smoothed frequency curve, while ticks indicate the actual
857 values.

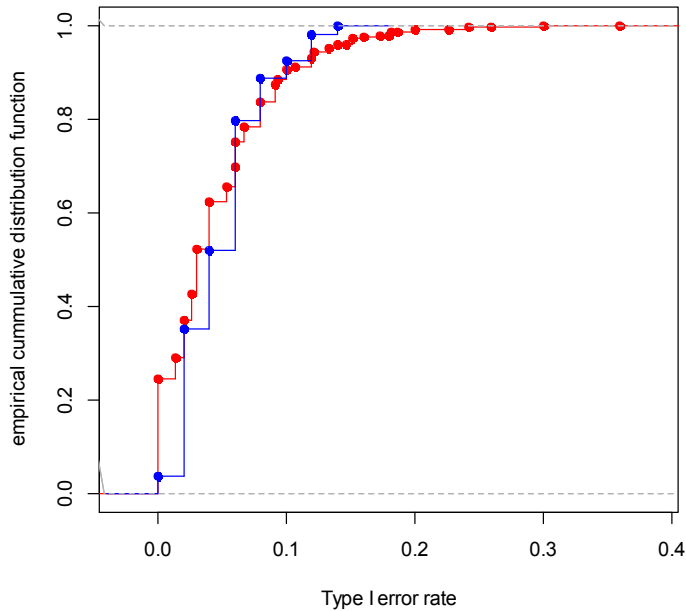


858

859 Figure S3.2 Distribution of trait B (related to competition) in the initial regional species pool (a), and
 860 three set of species pools after a simulation run with baseline values: trait values in the pool of
 861 observed species (b), and species occurring in the first (c) and last local community (d) along the
 862 environmental gradient. The line is a smoothed frequency curve, while ticks indicate the actual
 863 values.

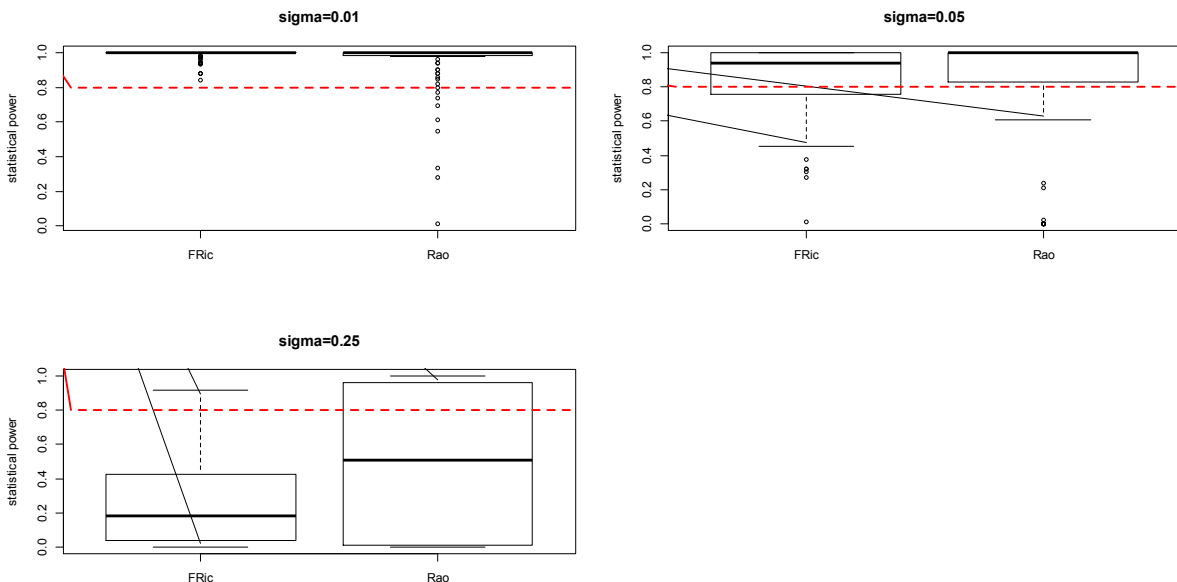
864

865 **Appendix S4:** Additional figures on the power of tests



866

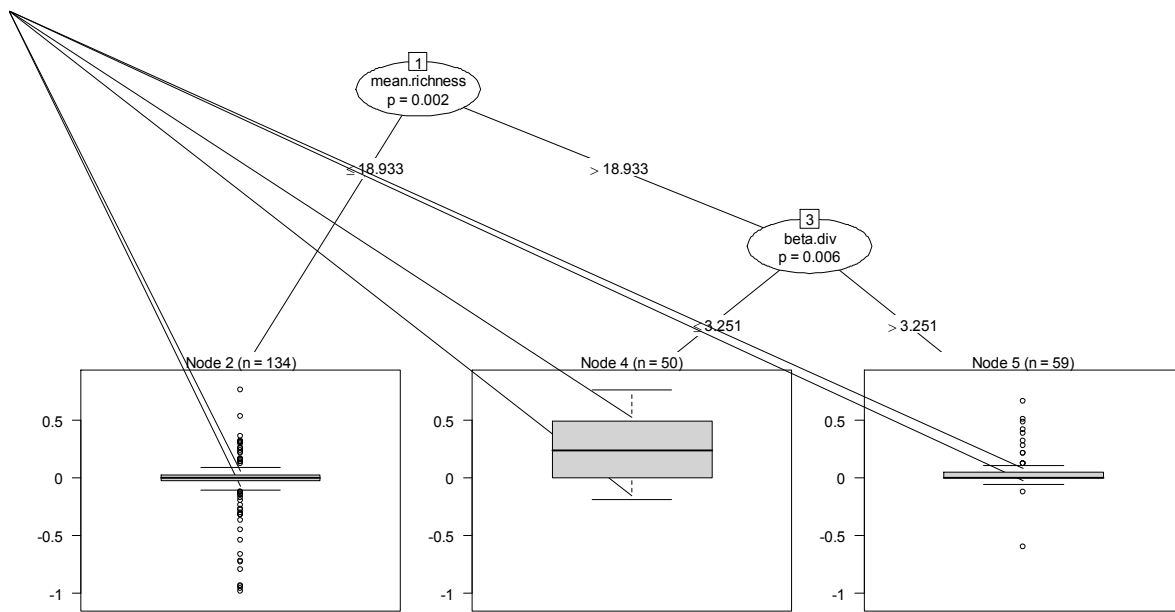
867 Figure S4.1 Empirical cumulative distribution function of type I error rate estimated by switching off
868 both habitat filtering and interspecific competition (blue lines and dots; n=54) and by using neutral
869 traits (red lines and dots; n=1437).



870

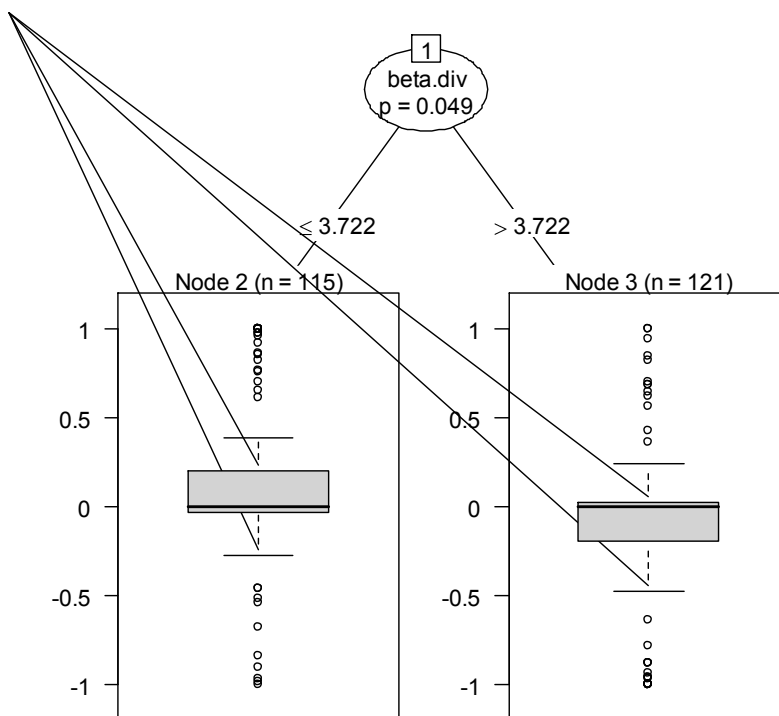
871 Figure S4.2 Power of the test for revealing trait convergence when applying between-plot
872 randomization strategy at three different levels of the strength of environmental filtering (lower
873 sigma means stronger filtering, see Figure S2.1).

874



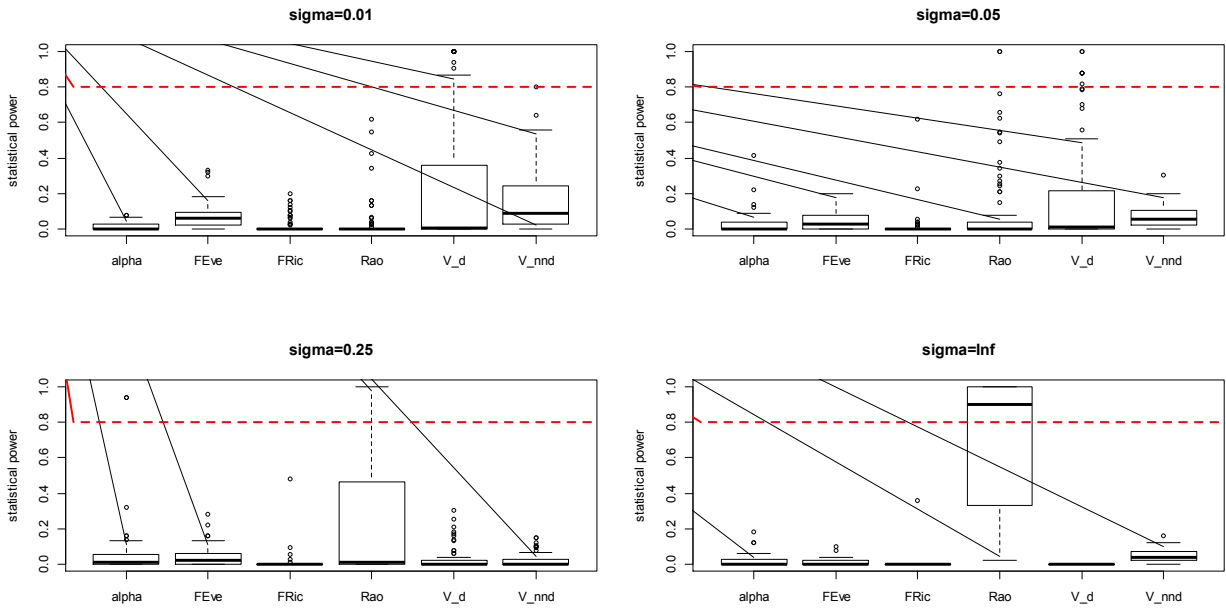
875

876 Figure S4.3 Conditional inference tree for differences in power between RaoQ and FRic for detecting
877 habitat filtering applying between-plot randomization. Positive values indicate that RaoQ performs
878 better.



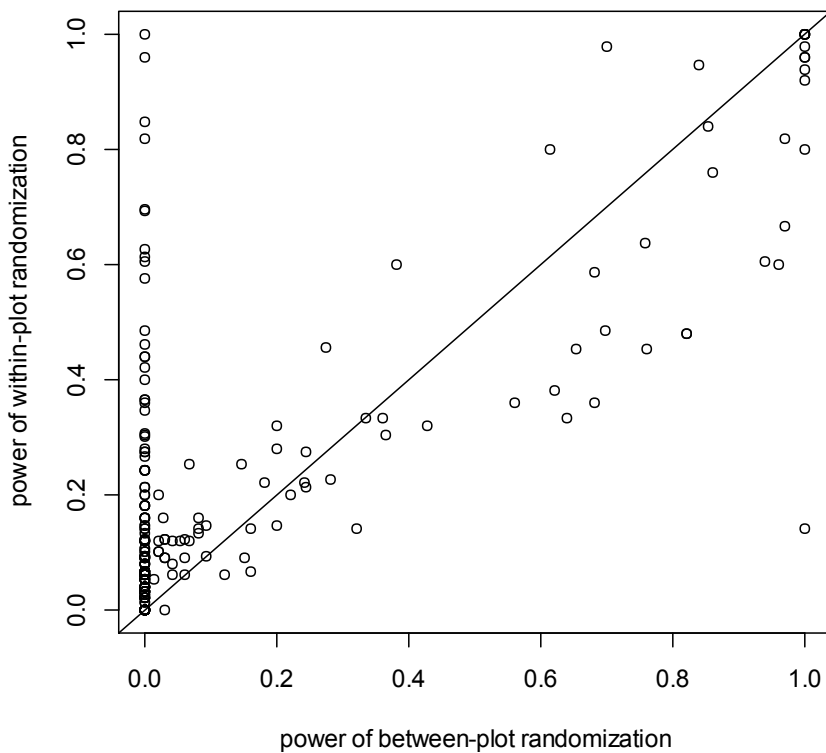
879

880 Figure S4.4 Conditional inference tree for differences in power between RaoQ and Vd for detecting
881 trait convergence applying between-plot randomization. Positive values indicate that RaoQ performs
882 better.



883

884 Figure S4.5 Power of trait divergence tests using between-plot randomization at four different levels
 885 of the strength of environmental filtering (lower sigma means stronger filtering).



886

887 Figure S4.6 Comparing the performance of tests using between- and within-plot randomization
 888 strategies for detecting trait divergence using *RaoQ* as test statistic.

889 **Appendix S5:** Dependence of the range of V_d on the range of trait values in one dimension

890 V_d is the variance of values in the lower (or upper) half-matrix of distance values. Let us denote the
 891 vector of these distance values by d . The length of this vector, hereafter denoted by n , depends on
 892 the number of species (S):

$$n = \frac{S(S-1)}{2}$$

893 Using these symbols the variance of distances can be calculated by the following form:

$$V_d = \left(\sum_{i=1}^n d_i^2 - \frac{(\sum_{i=1}^n d)^2}{n} \right) / (n-1)$$

894 Let us consider first the equidistant placing of species in range R . In this case the distance between
 895 neighbouring species is $\Delta = R/(S-1)$. In this case the possible distance values are: $\Delta, 2\Delta, 3\Delta, \dots, (S-j)\Delta, \dots,$
 896 $(S-1)\Delta$. The number of species pairs with these values are $S-1, S-2, S-3, \dots, S-j, \dots, 1$, respectively. Thus,

$$\begin{aligned} \left(\sum_{i=1}^n d \right)^2 &= \left(\sum_{j=1}^{S-1} (S-j)j\Delta \right)^2 = \Delta^2 \left(\sum_{j=1}^{S-1} (S-j)j \right)^2 = \frac{R^2}{(S-1)^2} \left(\sum_{j=1}^{S-1} (S-j)j \right)^2 \\ \sum_{i=1}^n d_i^2 &= \sum_{j=1}^{S-1} (S-j)j^2 \Delta^2 = \Delta^2 \left(\sum_{j=1}^{S-1} (S-j)j^2 \right) = \frac{R^2}{(S-1)^2} \left(\sum_{j=1}^{S-1} (S-j)j^2 \right) \\ V_d &= \frac{R^2}{(S-1)^2 n(n-1)} \left[n \left(\sum_{j=1}^{S-1} (S-j)j^2 \right) - \left(\sum_{j=1}^{S-1} (S-j)j \right)^2 \right] \end{aligned}$$

897 In this case, V_d equals the squared $FRic$ multiplied by a value that depends only on species richness.

898

899 When V_d is maximal, species are grouped into two clusters in the ends of trait gradients. The
 900 distances within groups are zero (i.e. species in the group has the same value), while the distance
 901 between groups is R . V_d is maximal, if the number of between-group distances, B , is as close to $n/2$
 902 as possible. The formulas for calculating depend on if S is even or odd, but value of B that maximizes
 903 V_d depends on S only. In this case:

$$\begin{aligned} \left(\sum_{i=1}^n d \right)^2 &= R^2 B^2 \\ \sum_{i=1}^n d_i^2 &= R^2 B \\ V_d &= R^2 \frac{nB - B^2}{n(n-1)} \end{aligned}$$

904 Again, V_d equals the squared $FRic$ multiplied by a value that depends only on species richness.
905 Between plot randomization does not change the species richness, but it can possibly change the
906 trait values and this way the possible minimum and maximum of V_d .
907

908 **Appendix S6:** Annotated R script for individual based simulation

```

909
910 #####
911 #                                                                 #
912 #           Community simulation                                 #
913 #                                                                 #
914 #####
915 #
916 # Input parameters:
917 #
918 # S = number of species in the regional species pool
919 # m = probability of colonization from meta-community
920 # n = number of local communities
921 # J = number of individuals in a local community
922 # sigma = tolerance width (equal for all species)
923 #       has to be positive
924 #       lower values means more specialist species
925 #       sigma=Inf means that species are maximally generalist,
926 #       thus abiotic conditions
927 #       do not influence their abundance
928 #       sigma=0 would mean that species are maximally specialist,
929 #       they can occur at only one point of the
930 #       environmental gradient(s)
931 # sigma.b = width of competition kernel
932 #       sigma.b=0 means no interspecific competition (no effect
933 #       of trait B on competition)
934 #       sigma.b=Inf leads to equally strong inter- and
935 #       intraspecific competition
936 # If both sigma and sigma.b equal to Inf, species are neutral,
937 # community composition influenced by random drift only
938 # b0 = probability of birth without competition
939 # K = carrying capacity
940 # xrange = the range of the environmental gradient, along which the
941 #       simulated sites lie
942 # distrib = parameter influencing the shape of distribution. It
943 #       should be positive!
944 #       distrib<1 U-shaped distribution
945 #       distrib=1 uniform distribution
946 #       distrib>1 bell-shaped distribution
947 # correl = correlation between traits, no ceorelation if correl=0
948 # (default)
949 # rand.seed = seed for random number generation
950 #       the default NULL initialize the random number
951 #       generator using current time
952 # sim.length = length of the simulation
953 #
954 #
955 #Output:
956 #
957 # List of parameters +
958 #       Y = plot-by-species matrix of abundances
959 #       trait.env, trait.compet, trait.neutr = three vector of
960 #       trait values
961
962 # S=200; m=0.1; n=50; J=300; sigma=0.05; sigma.b=0.03; b0=1;

```

```

963 # xrange=.8;distrib=1;
964 # correl=0;rand.seed=NULL; sim.length=100; K=200
965 # correl=-.6
966 # sigma = 0.05; sigma.b = 0.25; S = 200; J = 450; n = 50; distrib =
967 1; correl = 0; m = 0.1; b0 = 1; sim.length = 100; K = 200; xrange =
968 0.8; n.random = 1000; sig.level = 0.05
969 # rand.seed=NULL
970 traitsimul<-function(S=200, n=50, J=300, sigma=0.05, sigma.b=0.03,
971                      m=0.1, b0=1, xrange=.8, distrib=1, correl=0,
972                      rand.seed=NULL, sim.length=100, K=200, ...)
973 {
974   # the position of the sites along the environmental gradient:
975   # the xrange long central part of the gradient, sampled at
976   equidistant points
977   x <- seq((1-xrange)/2,1-(1-xrange)/2,xrange/(n-1))
978   set.seed(rand.seed)
979   cat("Generating species pool... \n")
980   trait.a <- rbeta(S, distrib, distrib) # values of trait1 (related
981   to tolerance)
982   tmp <- rbeta(S, distrib, distrib) # values of trait2 (related to
983   resource use)
984   trait.b <- switch(sign(correl)+2,
985     abs(correl)*(1-trait.a)+(1-abs(correl))*tmp, # correl: negative
986     tmp, # correl=0 (no
987     correlation)
988     correl*trait.a+(1-correl)*tmp) # correl:
989     positive
990   # correl values of +/- .6 result in cor(trait.a,trait.b) of ~.8 for
991   distrib=1 using this algorithm
992   trait.c <- rbeta(S, distrib, distrib) # values of trait3 (neutral)
993
994   dist.b <- as.matrix(dist(trait.b))
995   dist.a <- as.matrix(dist(trait.a))
996   compet <- matrix(0,S,S)
997   if (sigma.b==0) diag(compet) <- 1
998   if (sigma.b==Inf) compet <- matrix(1,S,S)
999   if ((sigma.b>0) & (sigma.b<Inf)) compet <- exp(-dist.b^2/sigma.b)
1000
1001
1002   Y<-matrix(NA,n,S) # species abundances
1003   off.spring<-vector()
1004   X<-matrix(rep(x,S),ncol=S) #position along the gradient
1005   A<-t(matrix(rep(trait.a,n),ncol=n))
1006
1007   survive <- if (sigma<Inf) pmax(exp(-((X-A)^2)/sigma)-0.01,0) else
1008   matrix(0.99,nrow(X),ncol(X))
1009
1010   cat("Generating starting community composition...\n")
1011   for (i in 1:n) Y[i,]<-
1012   table(c(sample(1:S,J,replace=T,prob=survive[i,]),seq(1,S)))-1
1013
1014   cat("Community assembly...\n")
1015   pb <- txtProgressBar (min = 0, max = sim.length, char = ".", width
1016   = 45, style = 3)
1017
1018   # epoch=1; j=1

```

```

1019   for (epoch in 1:sim.length) {
1020     for (j in 1:J) {
1021       seed<-matrix(0,nrow=n,ncol=S)
1022       for (i in 1:n) {
1023         death<-sample(1:S,1,prob=Y[i,])
1024         Y[i,death] <- Y[i,death]-1
1025         NE <- compet %*% Y[i,]
1026         birth.limit <- b0*(K-NE)/K
1027         birth.limit[birth.limit<0] <- 0
1028         occurrence <- (Y[i,]>0)
1029         seed[i,occurrence] <- rbinom(sum(as.numeric(occurrence)),
1030           Y[i,occurrence],birth.limit[occurrence])
1031       }
1032       off.spring <- matrix(rbinom(n*S,size=seed,prob=(1-
1033 m)),nrow=n,ncol=S)
1034       seed <- seed-off.spring
1035       p <- matrix(1/(n-1),nrow=n,ncol=n)
1036       diag(p) <- 0
1037
1038       for (i in 1:n)
1039         for (k in 1:S)
1040           if (seed[i,k]>0) off.spring[,k] <- off.spring[,k] +
1041             rmultinom(1, size=seed[i,k], prob=p[,i])
1042
1043       for (i in 1:n) {
1044         if (sum(off.spring[i,]*survive[i,])>0) {
1045           birth <- sample(1:S,1,prob=off.spring[i,]*survive[i,])
1046         } else {
1047           birth <- sample(1:S,1,prob=as.numeric(Y[i,]>0))
1048         }
1049         Y[i,birth] <- Y[i,birth]+1
1050       }
1051     }
1052     setTxtProgressBar(pb, epoch)
1053   }
1054   res <- list(S=S, m=m, n=n, J=J, sigma=sigma, sigma.b=sigma.b,
1055 b0=b0, x=x,
1056   distrib=distrib, correl=correl, rand.seed=rand.seed,
1057   sim.length=sim.length,K=K, Y=Y,trait.env=trait.a,
1058   trait.compet=trait.b,trait.neutr=trait.c)
1059   close(pb)
1060   return(res)
1061 }
1062

```